Calhoun: The NPS Institutional Archive
DSpace Repository

Theses and Dissertations 1. Thesis and Dissertation Collection, all items

1973

The far field analysis of parallel plate Luneberg Lenses for various feeds

Birchfield, Robert Boyd.

Monterey, California. Naval Postgraduate School

http://hdl.handle.net/10945/16616

Downloaded from NPS Archive: Calhoun

Calhoun is the Naval Postgraduate School's public access digital repository for research materials and institutional publications created by the NPS community. Calhoun is named for Professor of Mathematics Guy K. Calhoun, NPS's first appointed -- and published -- scholarly author.

Dudley Knox Library / Naval Postgraduate School
411 Dyer Road / 1 University Circle
Monterey, California USA 93943

http://www.nps.edu/library

THE FAR FIELD ANALYSIS OF PARALLEL PLATE LUNEBERG LENSES FOR VARIOUS FEEDS

Robert Boyd Birchfield

Library
Naval Postgraduate School
Monterey, California 93940

NAVAL POSTGRADUATE SCHOOL
Monterey, California

THESIS

THE FAR FIELD ANALYSIS
OF
PARALLEL PLATE LUNEBERG LENSES FOR VARIOUS FEEDS

by

Robert Boyd Birchfield

Thesis Advisor: R. W. Adler

September 1973

T156430

Approved for public release; distribution unlimited.

The Far Field Analysis
of
Parallel Plate Luneberg Lenses for Various Feeds

by

Robert Boyd Birchfield
Lieutenant, United States Navy
B.S., Purdue University, 1966
M.S., Naval Postgraduate School, 1973

Submitted in partial fulfillment of the
requirements for the degree of

ELECTRICAL ENGINEER

from the

NAVAL POSTGRADUATE SCHOOL
September 1973

Thesis
B5434
c.1

Library
Naval Postgraduate School
Monterey, 93940

ABSTRACT

This thesis developed expressions for the aperature fields and integral equations for the far field radiation characteristics of the Parallel Plate Luneberg Lens Microwave Antenna operating in the TEM or TE_{10} modes. These expressions were programmed on a digital computer to predict the far field radiation patterns for several feed systems. Experimentation produced far field radiation patterns that were very close to the theoretical patterns for the TE_{10} mode lens and substantially different for the TEM mode lens.

TABLE OF CONTENTS

I. INTRODUCTION - 7

II. THEORETICAL ANALYSIS - - - - - - - - - - - - - - - - - - 10

A. RAY PATHS - 11

B. APERATURE FIELD - - - - - - - - - - - - - - - - - - 13

C. ELECTROMAGNETIC FIELD CALCULATIONS - - - - - - - - - 18

III. EXPERIMENTAL VERIFICATION - - - - - - - - - - - - - - - - 22

A. DISCUSSION - 22

B. TE_{10} MODE LUNEBERG LENS - - - - - - - - - - - - - - 25

C. TEM MODE LUNEBERG LENS - - - - - - - - - - - - - - - 26

IV. CONCLUSIONS AND RECOMMENDATIONS - - - - - - - - - - - - 43

APPENDIX A: Ray Path Calculations - - - - - - - - - - - - - - 46

APPENDIX B: Electromagnetic Field Derivations - - - - - - - - - 50

APPENDIX C: Computer Programs - - - - - - - - - - - - - - - - 60

BIBLIOGRAPHY - 72

INITIAL DISTRIBUTION LIST - - - - - - - - - - - - - - - - - - 73

FORM DD 1473 - 74

LIST OF TABLES

Table No. Page No.

I. Theoretical and Experimental Curve Comparison ---------- 25

LIST OF FIGURES

Fig. No. Page No.

1. Focusing Properties of the Luneberg Lens ------------- 10
2. Geometry for Luneberg Lens Ray Path Derivation --------- 12
3. Ray Paths through Luneberg Lens ----------------------- 14
4. Geometry for the Derivation of the Aperature Fields ---- 15
5. Luneberg Lens Geometry Used in the Derivation of Radiation Expressions ---------------------------------- 19
6. Transmitter (X-Band) ---------------------------------- 23
7. Receiving/Pattern Recording System -------------------- 24
8. Waveguide Feed Pattern and Luneberg Lens Aperature Field 28
9. Luneberg Lens Far Field Radiation Patterns with Waveguide Feed -- 29
10. Luneberg Lens (TE_{10} mode) H-Plane Far Field Patterns for Waveguide Feed --------------------------------------- 30
11. Luneberg Lens E-Plane Patterns for Waveguide Feed at 7.0 GHz --- 31
12. Luneberg Lens E-Plane Patterns for Waveguide Feed at 8.0 GHz --- 32
13. Luneberg Lens E-Plane Patterns for Waveguide Feed at 9.0 GHz --- 33
14. Luneberg Lens E-Plane Patterns for Waveguide Feed at 10 GHz -- 34
15. Luneberg Lens E-Plane Patterns for Waveguide Feed at 11 GHz -- 35
16. Yagi Array Feed Pattern and Luneberg Lens Aperature Field for Yagi Feed ------------------------------------ 36
17. Luneberg Lens (TE_{10} mode) E-Plane Patterns for Yagi Feed at 10 GHz ------------------------------------- 37
18. TEM Mode Luneberg Lens Theoretical E-Plane Radiation Patterns with Waveguide Feed at 10 GHz --------------- 38

Fig. No. Page No.

19. Dielectric Loaded Sectoral Horn Feed Patterns and Aperature Field for Sectoral Horn Feed ---------------- 39

20. TEM Mode Luneberg Lens Theoretical E-Plane Radiation Patterns for Sectoral Horn Feed at 10 GHz ------------- 40

21. TEM Mode Luneberg Lens Experimental E-Plane Pattern for Sectoral Horn Feed at 10 GHz ---------------------- 41

22. TEM Mode Luneberg Lens H-Plane Radiation Patterns for Sectoral Horn Feed at 10 GHz --------------------------- 42

23. Geometry for Luneberg Lens Ray Path Derivations -------- 47

24. Luneberg Lens Geometry Used in the Derivation of Radiation Expressions --------------------------------- 51

I. INTRODUCTION

Theoretical work by R.K. Luneberg [Ref. 1] on optics in a medium of variable index of refraction resulted in the development of the Luneberg Lens which has many applications in microwave antennas. Two of the most common Luneberg Lenses are of the spherical and cylindrical types, in which the index of refractions is a function of radius only. In these lenses, the index of refraction is varied so that the radiation from a point source placed at the edge of the lens produces a collimated beam on the opposite side of the lens. The index of refraction is 1.0 at the edge of the lens so that it is matched to free space.

Spherical or cylindrical Luneberg Lenses are constructed by bonding concentric dielectric shells or hoops together, or by a special mixing and blending process which produces a continuously varying index of refraction as a function of the radius [Ref. 2]. Cylindrical lenses are also produced by taking a cylinder of dielectric material and machining one surface until the required average index of refraction, when placed between two parallel plates, is achieved.

Cylindrical Luneberg Lenses operate in either the TEM or the TE_{10} modes. If the thickness of the lens is greater than one-half wavelength but less than one wavelength, it operates in the TE_{10} mode. However, if the lens is several wavelengths thick it will operate in the TEM mode.

Many radar systems and most electronic warfare systems require antennas that can scan a narrow beam over wide angles in space. As long as the scan rates are low, the present rotating systems are adequate. However, when the required scan rates are increased or the application

requires instantaneous repositioning of the beam, rotating antennas cannot fulfill the requirements due to their inertia. It can be shown that for some passive electronic warfare systems the optimum scan rates are in excess of 3000 rpm. In addition to this, the beamwidth of present rotating antenna systems are too wide to permit the desired accuracy in the determination of the direction of arrival of an intercepted signal.

A new antenna system is therefore required to more fully utilize the capabilities of current equipment. The Luneberg Lens has the potential to overcome the above deficiencies and, in addition, provide a higher gain and reduce the weight of heavy antenna systems placed on the superstructure of ships. In view of this potential, this thesis was designed to analyze the parallel plate, continuously varying dielectric, cylindrical Luneberg Lens. The analysis was to produce theoretical expressions for the far field radiation patterns of the lens for any feed system. This would provide a method of determining the performance of any size lens with any feed system to be investigated without going to the expense of buying or constructing a lens and measuring the far field radiation patterns. The only requirement is that the radiation patterns of the feed system be known. The feed system patterns may be known functions or they may be measured. The far field expressions were programmed on the IBM 360 computer to compute and plot the far field radiation patterns. The accuracy of this analysis was verified experimentally.

Although the analysis of the Luneberg Lens was carried out for arbitrary feed polarization, lens size, and frequency, some limits had to be placed upon the experimentation. The experimental limitations were: (1) feed systems polarized in a plane perpendicular to the plane of the lens, (2) the far field radiation patterns of the feeds were used in

calculating the far field expressions of the Luneberg Lenses, (3) all the experimentation was confined to x-band due to availability of equipment, and (4) a "roof-top" range was used for some measurements.

II. THEORETICAL ANALYSIS

Electromagnetic energy propagating through a lens follows optical ray paths [Ref. 3]. In the case of the radially-symmetric, cylindrical Luneberg Lens, the optical ray paths are such that the energy from an incident plane wave is focused into a cylindrical wave front on the surface of the lens diametrically opposite the direction of incidence as indicated in Fig. 1.

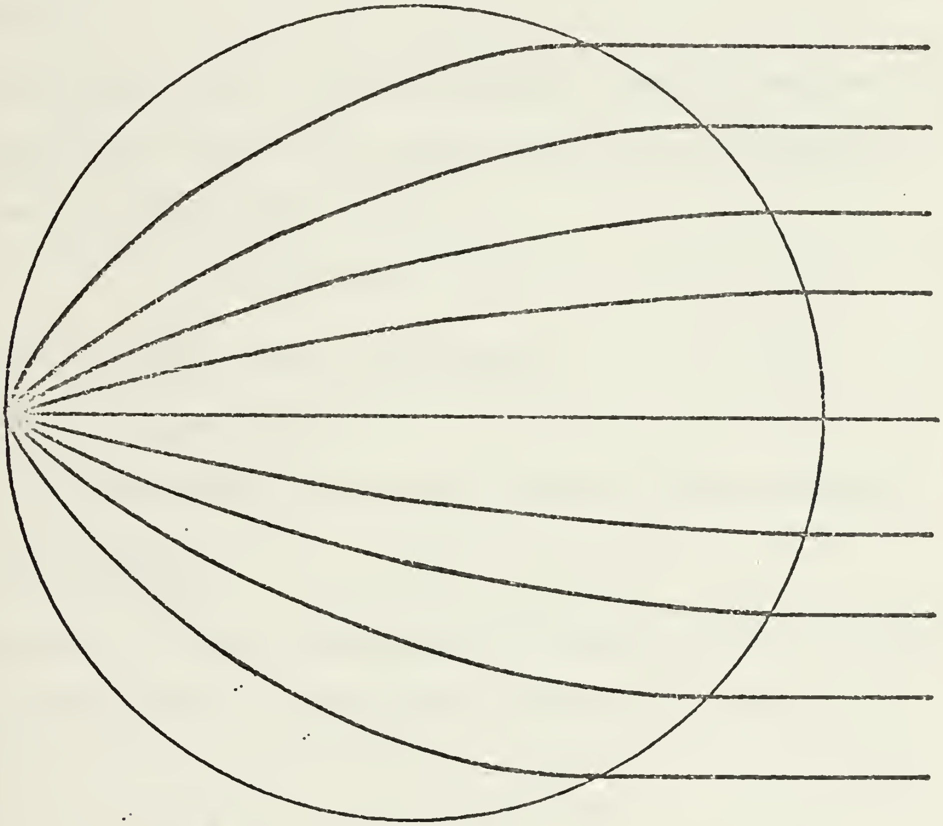

Figure 1. Focusing Properties of the Luneberg Lens.

The refraction necessary to achieve this focusing effect is obtained by properly varying the index of refraction. In the cylindrical Luneberg Lens the index of refraction, n(r) is given by

$$n(r) = \sqrt{2 - (r/r_o)^2}, \tag{1}$$

where r is any radius and r_o is the radius of the lens. Thus the index of refraction varies from $\sqrt{2}$ at the center of the lens to 1.0 at the edge.

The theoretical analysis of the Luneberg Lens is based upon the principles of geometric optics from which the Ray Paths and the Aperature Field of the Lens are calculated and plotted. The far field radiation patterns are then calculated from the Aperature Field.

A. RAY PATHS

The generalized Snell's Law for circular symmetry, such as is present in the cylindrical Luneberg Lens, where the index of refraction is a function of the radius only [Ref. 3] is:

$$n(R) \sin \Theta = C_1 , \tag{2}$$

where $n(R) = \sqrt{2-R^2}$ = index of refraction,

R = normalized radius,

Θ = angle between the ray path and the outward meridian,

C_1 = constant.

The geometry of Fig. 2 and equation (2) were utilized to derive an integral formula[1] for the relationship between R, Ψ, and C_1.

$$\Psi = C_1 \int \frac{1}{R} [-R^4 + 2R^2 - C_1^2]^{-1/2} dR , \tag{3}$$

where Ψ is the angle between the direction of arrival of the plane wave and the radius through a point on the ray. A unique ray exists for each value of C_1 ($0.0 \leq C_1 \leq 1.0$).

---

[1] For complete derivation see Appendix A.

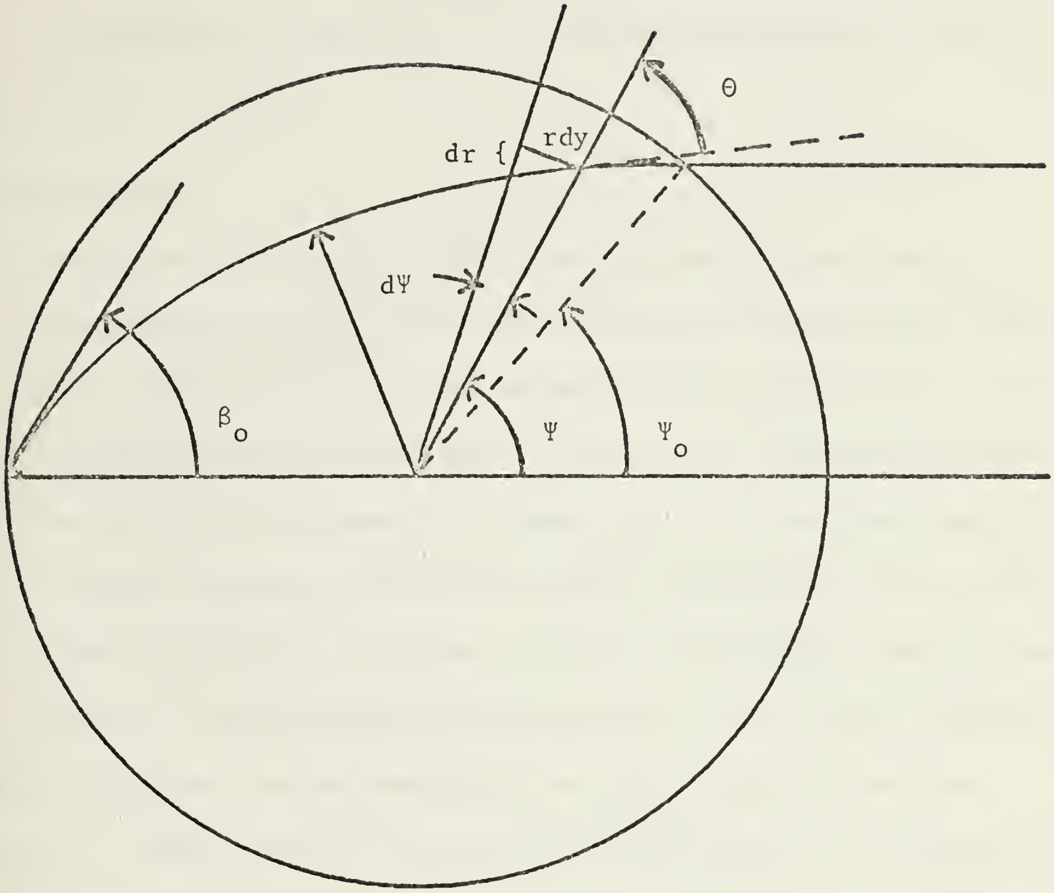
Θ
dr {
rdy
dΨ
β₀
Ψ
Ψ₀

Figure 2. Geometry for Luneberg Lens Ray Path Derivation.

Equation (3) was separated into two intervals as given by equations (41) and (42) of Appendix A and programmed for the IBM 360 computer. The ray path plots are given in Fig. 3 for ten values of C_1. Note that β_o was equal to Ψ_o and that the closest point of approach to the origin by a ray (r_m) occured for Θ equal to 90°. Each ray is symmetric about the point ($r = r_m$, $\Theta = 90°$).

B. APERATURE FIELD

The relationship between the Feed Distribution and the Aperature Field of the Luneberg Lens was derived utilizing the principles of geometric optics, for the geometry and variables defined in Figure 4. The energy flow into a Differential Element $d\beta dx$ must be identical to the energy flow out of the Differential Element $dxdy$, since from the principles of Geometric Optics it has been shown in section II-A that energy flow is along Ray Paths. If a tube of rays is considered, then the energy flow is constant through various cross-sections of the tube. Therefore, the energy flow into the wedge-shaped tube, $d\beta dx$, at the feed is $S_1(\beta,x)d\beta dx$, where $S_1(\beta,x)$ is the energy distribution per unit angle in the primary feed pattern.

Equating the energy that enters the flux tube, $d\beta dx$, to the energy leaving the flux tube, $dxdy$, $S_a(x,y)\,dxdy = S_1(x,\beta)\,d\beta dx$, where $S_a(x,y)$ is the energy in the lens aperature. However, $S_a(x,y)$ is proportional to $|E'_a|^2$, where $|E'_a|$ is the magnitude of the electric field in the aperature. Therefore,

$$S_a(x,y)dxdy = C_2|E'_a|^2 dxdy = S_1(x,\beta)d\beta dx \qquad (4)$$

where C_2 is a constant. From the geometry of Figure 4

$$y = r_o \sin \Psi \qquad (5)$$

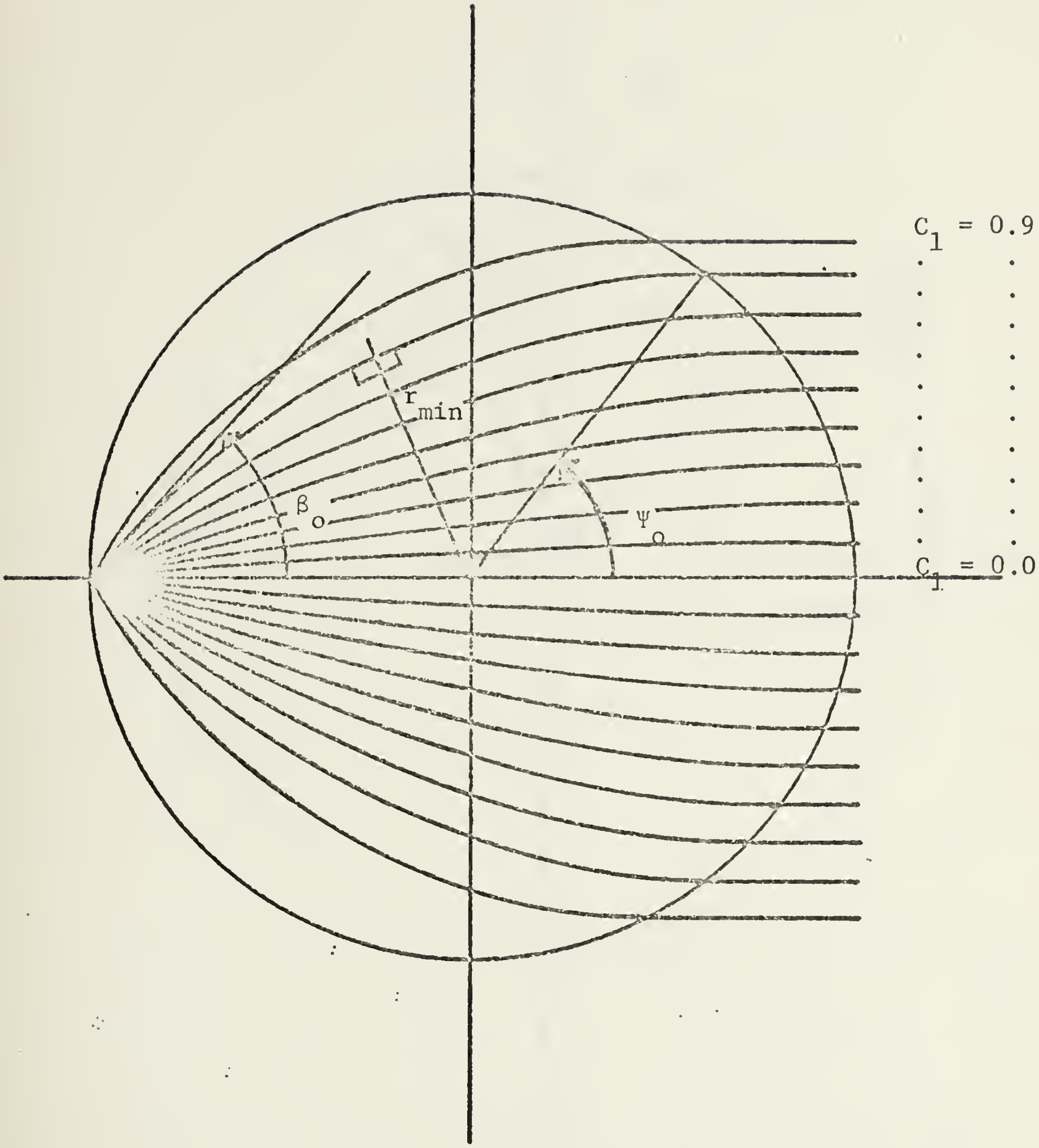
$C_1 = 0.9$
r_{min}
β_o
Ψ_o
$C_1 = 0.0$

Figure 3. Ray Paths Through Luneberg Lens.

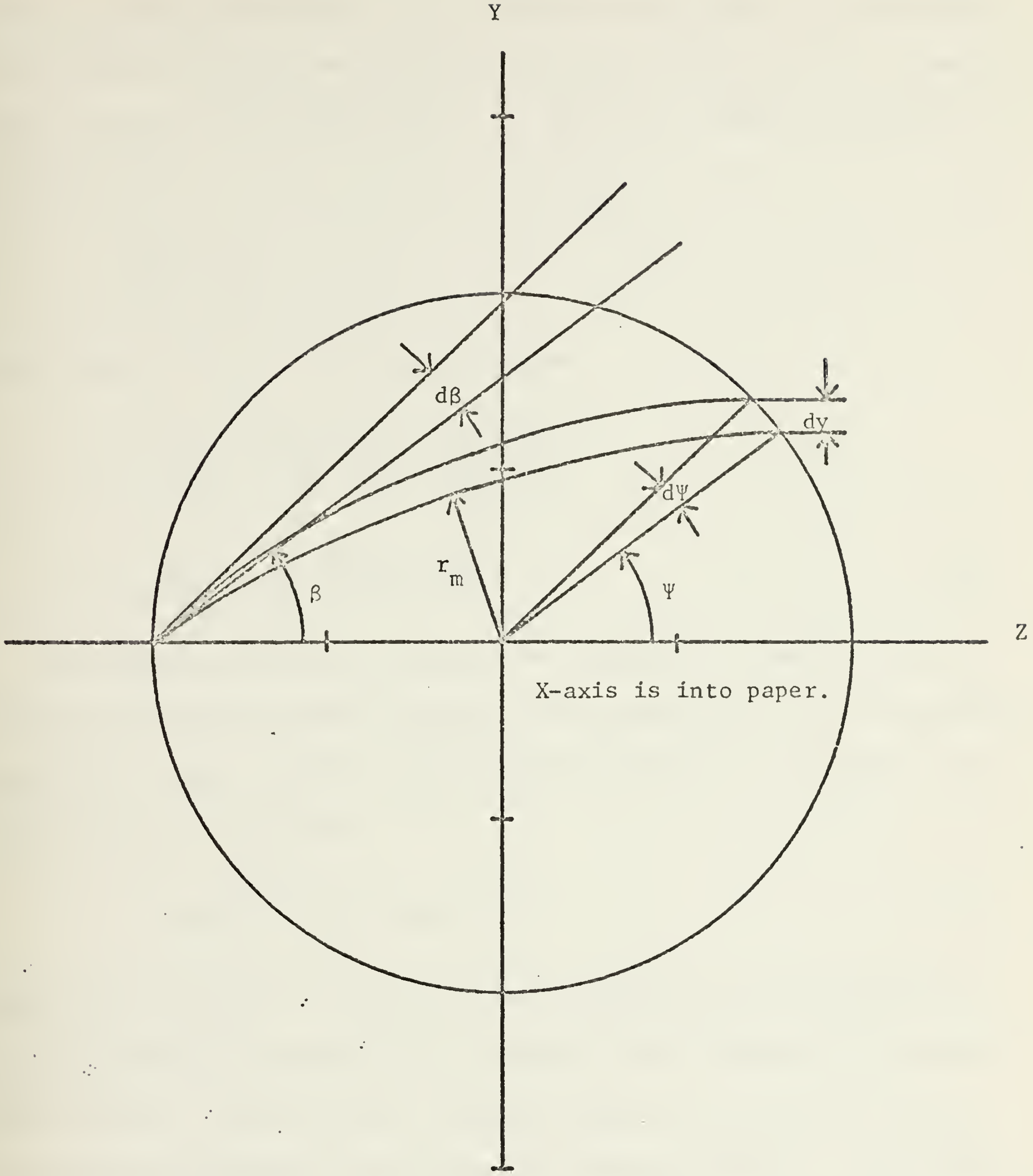
Y
Z
dβ
dy
dΨ
r_m
β
Ψ
X-axis is into paper.

Figure 4. Geometry for the Derivation of the Aperature Fields.

where r_o is the lens radius. r_m is defined as the point on a ray nearest the origin, and due to the symmetry of the Lens, the ray path is symmetric about the point $r = r_m$ and hence $\Psi = \beta$ [Ref. 4]. Then from equation (5) and this fact

$$\frac{dy}{d\Psi} = \frac{dy}{d\beta} = r_o \cos \Psi .$$

Substituting this into equation (4) yields

$$|E'_a|^2 = \frac{S_1(x,\beta)}{C_2} \frac{d\beta}{dy} = \frac{S_1(x,\Psi)}{C_2 r_o \cos \Psi}$$

or

$$|E'_a| = C_3 \sqrt{S_1(x,\Psi) \sec \Psi} \tag{6}$$

The Aperature field can therefore be calculated for any feed distribution for either the TEM or the TE_{10} mode Luneberg Lens. Two assumptions were made. First, that the feed energy distribution is a separable function of x and Ψ. Therefore

$$S_1(x,\Psi) = S_2(x)\, S_3(\Psi). \tag{7}$$

The second assumption is that $S_2(x)$ and $S_3(\psi)$ can be calculated or approximated from the geometry or by computer curve fitting of a measured feed pattern. For either type Luneberg Lens the S_3 (ψ) can be equated to the feed distribution in the plane of the lens [Ref. 4]. $S_2(x)$, however, is different for each type of lens and is a function of the lens geometry. In the TE_{10} mode lens as is suggested from wave guide theory

$$[S_2(x)]_{TE_{10}} \propto \cos \left(\frac{x}{a}\right), \tag{8}$$

where a is the thickness of the lens. In the TEM mode lens the assumption

was made that the $S_2(x)$ is constant over the x-dimension of the lens, and

$$[S_2(x)]_{TEM} \propto C_4. \tag{9}$$

The Luneberg Lens was designed to produce a constant phase in the plane of the lens along a line tangent to the aperature center; therefore, the aperature fields have a phasing

$$kr_o(1 - \cos \Psi). \tag{10}$$

Then for the Luneberg Lens

$$E'_a = |E'_a| \, e^{jkr_o(1 - \cos \Psi)} . \tag{11}$$

Combining equations (6), (7), and (9) for the TEM mode Luneberg Lens,

$$E'_a \propto \sqrt{S_3(\Psi) \sec \Psi} . \tag{12}$$

However, $S_3(\Psi) \propto (E'_a(\Psi))^2$, so that

$$E'_a(x,\Psi) = C_5 E_a(\Psi) \sqrt{\sec \Psi} , \tag{13}$$

where C_5 is a constant of proportionality and $E_a(\Psi)$ is the magnitude of the feed distribution. Rewriting with the phasing information of equation (10),

$$E'_a(x,\Psi) = C_5 E_a(\Psi) \sqrt{\sec \Psi} \, e^{jkr_o(1 - \cos \Psi)} . \tag{14}$$

Combining equations (6), (7), and (8) for the TE_{10} mode Luneberg Lens the aperature field is

$$E'_a \propto |E'_a| \sqrt{S_3(\Psi) \sec \Psi} \cos \left(\frac{x}{a}\right)$$

or

$$E'_a(x,\Psi) = C_6 \cos \left(\frac{x}{a}\right) E_a(\Psi) \sqrt{\sec \Psi} \, e^{jkr_o(1 - \cos \Psi)} . \tag{15}$$

C. ELECTROMAGNETIC FIELD CALCULATIONS

The Electric Field of the Luneberg Lens was calculated utilizing the aperature field method and Huygens Principle as developed in Chapter 2 of Ref. 5. The Electric Field equations are:

$$\overline{E} = -\frac{1}{\varepsilon}\,\overline{\nabla} \times \overline{F} - \frac{j}{\omega\mu\varepsilon}\,\overline{\nabla} \times \overline{\nabla} \times \overline{A}, \tag{16a}$$

and

$$\overline{H} = \frac{1}{\mu}\,\overline{\nabla} \times \overline{A} - \frac{j}{\omega\mu\varepsilon}\,\overline{\nabla} \times \overline{\nabla} \times \overline{F} \tag{16b}$$

where

$$\overline{A} = \frac{\mu}{4\pi}\iint \overline{J}(x',\Psi')\frac{e^{-jkR}}{R}\,dS' , \tag{17}$$

$$\overline{F} = \frac{\varepsilon}{4\pi}\iint \overline{K}(x',\Psi')\frac{e^{-jkR}}{R}\,dS' , \tag{18}$$

$$\overline{J}(x',\Psi') = \overline{n} \times \overline{H}_a , \tag{19}$$

$$\overline{K}(x',\Psi') = \overline{E}_a \times \overline{n} , \tag{20}$$

$$dS' = \rho\ dx'd\Psi' , \tag{21}$$

$$k = \frac{2\pi}{\lambda} , \tag{22}$$

and the remaining variables are shown in Fig. 5. Only the Electric Field will be considered from this point since the Far-Field is essentially a plane wave, where E and H are related by the intrinsic impedance of Free-Space.

The Far-Field equations[2] derived from equations (16-22) and the geometry of Fig. 5 for a feed polarized in the x-direction are:

---

[2] See Appendix B for derivation.

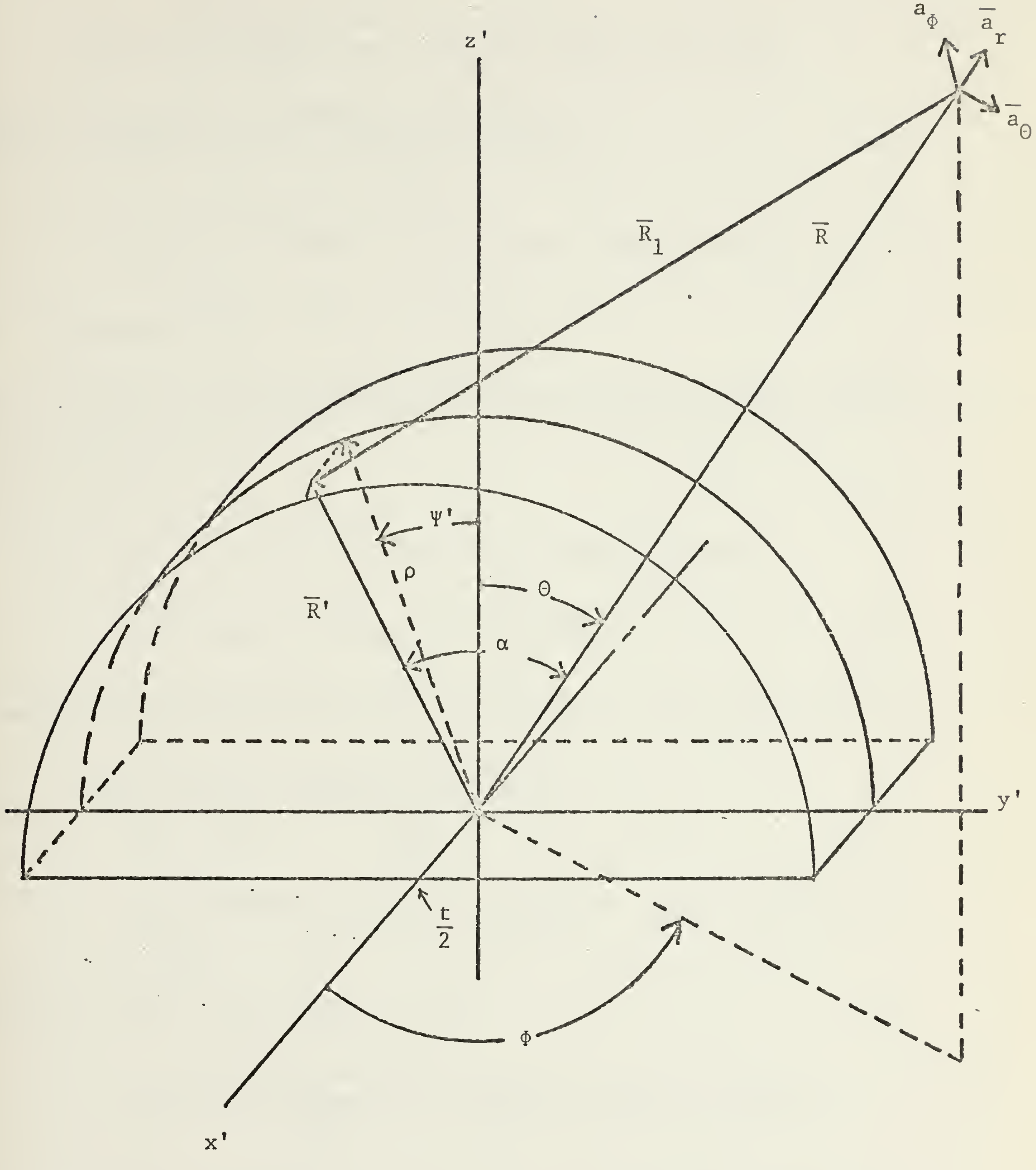

$\overline{a}_\Phi$
$\overline{a}_r$
$\overline{a}_\Theta$
z'
$\overline{R}_1$
$\overline{R}$
Ψ'
ρ
$\overline{R}'$
Θ
α
y'
$\frac{t}{2}$
Φ
x'

Figure 5. Luneberg Lens Geometry Used in the Derivation of Radiation Expressions.

$$\overline{E}_{\Theta}(R,\Phi,\Theta) = \frac{jk\rho\ e^{jk\rho}}{4\pi}\ [1 - \cos\Theta][\cos\Phi] \tag{23}$$

$$\iint \left[\frac{e^{-jk|R_1|}\ e^{-jk\rho\cos\Psi'}}{|R_1|}\right][E_{ax}(x',\Psi')\cos\Psi']\ dx'\ d\Psi',$$

$$E_{\Phi}(R,\Phi,\Theta) = \frac{jk\rho\ e^{jk\rho}}{4\pi}\iint \left[\frac{e^{-jk|R_1|}\ e^{-jk\rho\cos\Psi'}}{|R_1|}\right] \tag{24}$$

$$[E_{ax}(x',\Psi')][\sin\Theta\sin\Psi' - \cos\Psi'\sin\Phi(1+\cos\Theta)]dx'\ d\Psi',$$

and $\quad E_R(R,\Phi,\Theta) = 0;$ (25)

where $E_{ax}(x',\Psi\ )$ is the magnitude of the Lens aperature field polarized in the x-direction and

$$R_1 = [R^2 + (x')^2 + \rho^2 + 2R(x'\cos\Theta\cos\Phi - \rho\sin\Psi'$$

$$\sin\Theta\sin\Phi + \rho\cos\Psi'\cos\Theta)]^{1/2}. \tag{26}$$

The far-field equations for a feed polarized in the y-direction are:

$$\overline{E}\ (R,\Phi,\Theta) = \frac{jk\rho\ e^{jk\rho}}{4\pi}\iint \left[\frac{e^{-jk|R_1|}\ e^{-jk\rho\cos\Psi'}}{|R_1|}\right] \tag{27}$$

$$[E_{ay}(x',\Psi')][\cos\Psi'\sin\Phi\ (1+\cos\Theta\ ) - \sin\Theta\sin\Psi']dx'\ d\Psi',$$

$$E\ (R,\Phi,\Theta) = \frac{jk\rho\ e^{jk\rho}}{4\pi}\ [\cos\Phi(\cos\Theta + 1)] \tag{28}$$

$$\iint \left[\frac{e^{-jk|R_1|}\ e^{-jk\rho\cos\Psi'}}{|R_1|}\right][E_{ay}(x',\Psi')\cos\Psi']\ dx'\ d\Psi',$$

and $\quad E_R(R,\Phi,\Theta) = 0;$ (29)

where $E_{ay}(x',\Psi')$ is the magnitude of aperature field polarized in the y-direction and $|R_1|$ is as given in equation (26).

The Far-Field radiation patterns are identical as can be seen by comparing equations (23) and (24) to equations (28) and (27) respectively. Due to this identity, the Far-Field radiation patterns are independent of the Feed Polarization. Therefore, only one set of equations need be utilized in calculating and plotting the far-field radiation patterns for any feed polarization in the x-y plane.

Approximating $\frac{1}{|\overline{R}_1|}$ by $\frac{1}{|\overline{R}|}$ and $|\overline{R}_1|$ by $|\overline{R}| - |\overline{R}' \cdot \overline{a}_r|$ (far field condition)[3] then equations (13) and (14) become:

$$E_\Theta = \frac{jk\rho}{4\pi R}[1 - \cos\Theta][\cos\Phi]e^{jk(\rho - R)} \int e^{CEX} E_{a_1}(x)\, dx \int e^{CER} \cos\Psi E_{a_1}(\Psi)\, d\Psi$$

and (30)

$$E_\Phi = \frac{jk\rho}{4\pi R} e^{jk(\rho - R)} \int e^{CEX} E_{a_1}(x)\, dx \int e^{CER} \cos\Psi E_{a_1}(\Psi)$$

$$[\sin\Theta \sin\Psi - \cos\Theta \sin\Phi \cos\Psi - \sin\Phi \cos\Psi]\, d\Psi\ , \qquad (31)$$

where $CEX = jkx \sin\Theta \cos\Phi$ (32)

and $CER = jkP(\cos\Psi \cos\Theta - \sin\Psi \sin\Theta \sin\Phi - \cos\Psi)$. (33)

Equations (30) and (31) were programmed for the IBM-360 computer for calculating and plotting the normalized far-field radiation patterns. The computer programs are given in Appendix C, and the theoretical far-field radiation patterns are given in Section III.

---

[3] Calculations show that for the worst condition ($\Psi = 90°$) at a distance of $2L^2/\lambda$ the phasing error is less than $.06\lambda$ (21°).

III. EXPERIMENTAL VERIFICATION

A. DISCUSSION

Experimental verification was undertaken to determine the validity of the equations that describe the far-field radiation patterns of the Parallel-Plate Luneberg Lenses. In order to accomplish this, two Luneberg Lenses were acquired. One was a TEM mode lens, 44 inches (37.2 λ at 10 GHz) in diameter and 2.38 inches thick. The other was a TE_{10} mode lens, 10.25 inches (8.67λ at 10 GHz) in diameter and 0.5 inches thick. All measurements were made with the lenses operating in the receive mode and for far-field conditions (distance > $2L^2/\lambda$). Measurements on the TE_{10} mode lens were conducted in an anechoic chamber and those for the TEM mode lens were conducted in a "roof-top" range. The transmitting set-up is shown in Fig. 6, and was operated in the CW mode at 10 GHz. The only exception was for a frequency characteristics check of the TE_{10} mode lens. The receiving set-up is given in Fig. 7.

The procedure followed was to measure the far-field patterns of the feed and the Luneberg Lens and then using the feed data, calculate the far-field patterns and compare the two results.

It was noted that in the case of all feeds with both lenses that when the feed was placed very close to the lens the first side lobes almost merged into the main beam. As the distance between the feed and lens increased the side lobes became distinct and dropped very rapidly. Then the particular placement of the feed was found which resulted in optimum (lowest) side lobe levels. When the separation was increased to a distance greater than the optimum, the main beam spread out and engulfed the first side lobes.

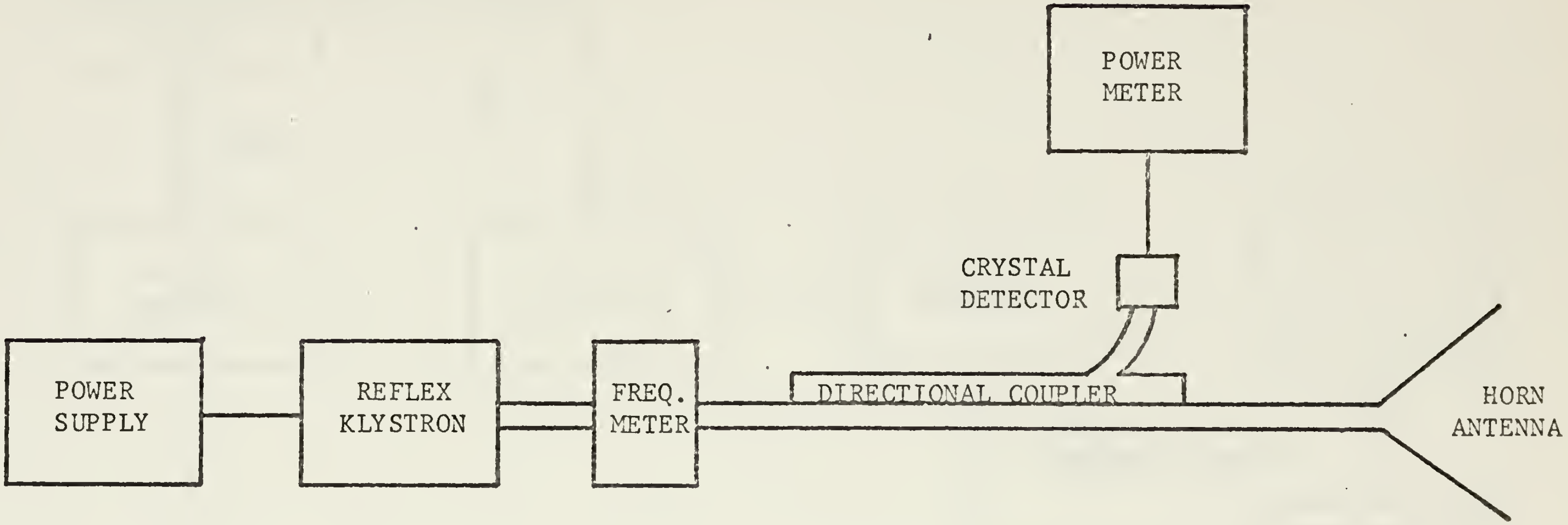
POWER
METER
CRYSTAL
DETECTOR
POWER
SUPPLY
REFLEX
KLYSTRON
FREQ.
METER
DIRECTIONAL COUPLER
HORN
ANTENNA

Figure 6. Transmitter (X-Band).

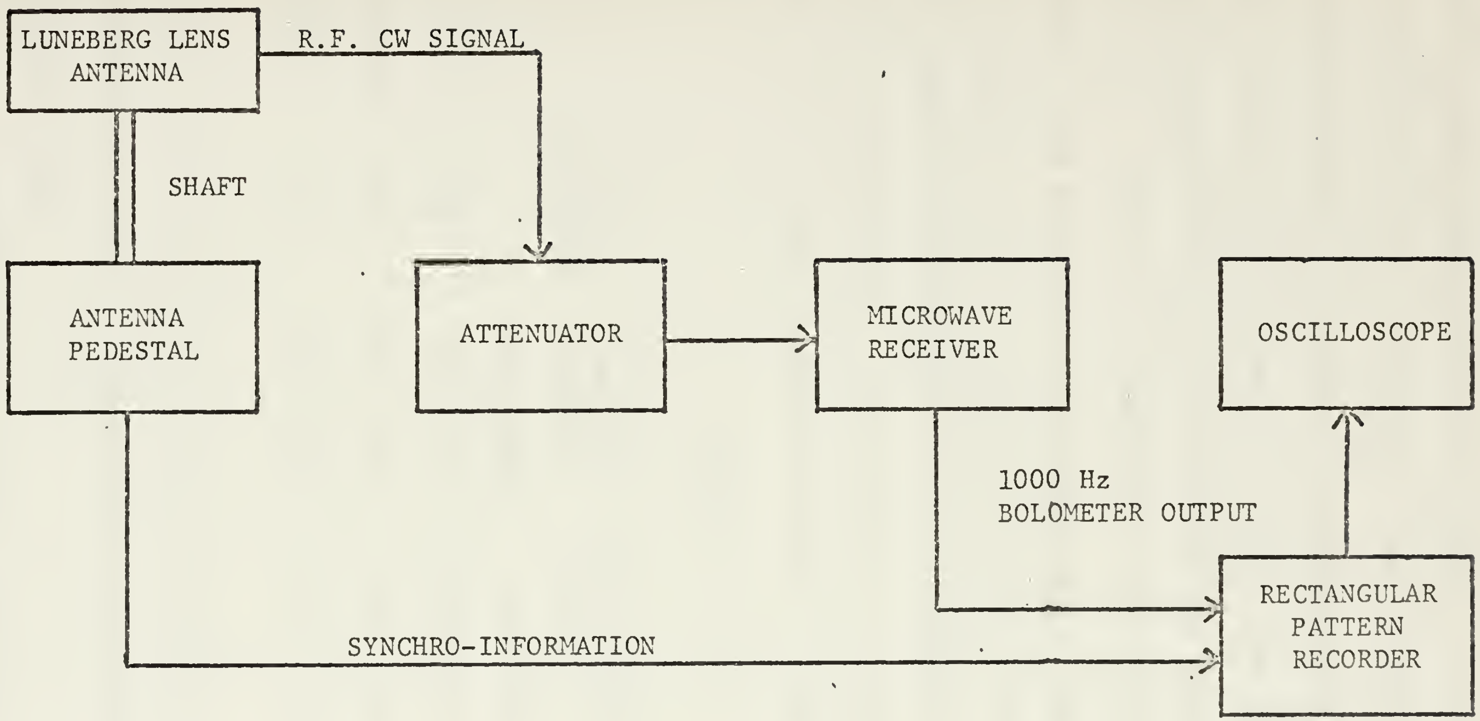
LUNEBERG LENS ANTENNA
R.F. CW SIGNAL
SHAFT
ANTENNA PEDESTAL
ATTENUATOR
MICROWAVE RECEIVER
OSCILLOSCOPE
1000 Hz BOLOMETER OUTPUT
RECTANGULAR PATTERN RECORDER
SYNCHRO-INFORMATION

Figure 7. Receiving/Pattern Recording System.

B. TE_{10} MODE LUNEBERG LENS

The TE_{10} Mode Luneberg Lens was fed by two different feed systems. The first was an "open-end" waveguide feed (hereafter referred to as the waveguide feed) and the other was a two element Yagi array (driven element plus director) resonant at 10 GHz. The far field patterns of the lens aperature fields for these feeds are given in Figures 8 and 16 respectively. Fig. 9 is a comparison of the theoretical vs. the experimental far field patterns in the planes of the lens (E-plane), when fed by the waveguide feed at a frequency of 10 GHz. The gain over isotropic of this system is approximately 20 db, as compared to a 16 db standard horn, with a one-half power beam width of 6.5 degrees. The salient points of the two curves are given in Table I, below.

TABLE I

	3 db Beam Width	First Null Location		First Sidelobe Location		First Sidelobe Amplitude (db)	
		left	right	left	right	left	right
Theoretical	6.8°	-8.2°	8.3°	-10.8°	10.6°	-19.6	-19.6
Experimental	6.5°	-7.4°	7.8°	- 9.9°	10.3°	-17.9	-18.2
Difference	0.3°	0.6°	0.5°	0.9°	0.3°	1.7	1.4

Figure 10 is a comparison of the theoretical and experimental H-plane (perpendicular to plane of lens at beam center) far field patterns for the waveguide feed.

In order to determine the frequency characteristics of the TE_{10} mode lens when fed by the waveguide, feed far field patterns for 7,8,9 and 11 GHz were also calculated and are presented in Figures 11 and 15. The

experimental far field patterns were different from the theoretical patterns by about the same amount as the patterns at 10 GHz.

The experimental vs. theoretical E-plane far field patterns of the TE_{10} Mode Lens fed by the Yagi feed are given in Fig. 17. The differences in side lobe and null locations and side lobe levels are negligible. The gain over isotropic of this arrangement is about 21.5 db as compared to the 16 db standard gain horn, with a one-half power beam width of 6.2 degrees.

A comparison of the lens aperature fields (Figures 8 and 16) show that the Yagi array feed utilizes the lens aperature more efficiently than the waveguide feed.

C. TEM MODE LUNEBERG LENS

The theoretical and experimental E-plane far field patterns of the TEM Mode Luneberg Lens when fed with a dielectrically loaded sectoral horn feed (feed pattern and lens aperature field given in Fig. 19) are given in Figures 20 and 21, respectively. The difference between these two patterns is about 1.0 degrees in the one-half power beam width, 0.5 degrees in the first null placement, 2.5 degrees in the first sidelobe placement, and 8.0 db in first sidelobe amplitudes. The gain over isotropic of this arrangement was about 25 db. The theoretical H-plane far field pattern is given in Fig. 22. The 3 db theoretical H-plane beam width is 22 degrees as compared to 25.5 degrees obtained experimentally by the Naval Electronic Laboratory Center [Ref. 2].

When the TEM mode lens was fed by the waveguide feed (Fig. 8) the theoretical (Fig. 18) and the experimental far field pattern differences were somewhat less that they were for the sectoral horn, but due to range difficulties reliable experimental patterns were not obtained.

It is felt that the differences between the theoretical and experimental patterns were too great to warrant further investigation without refinement of the feed systems analysis.

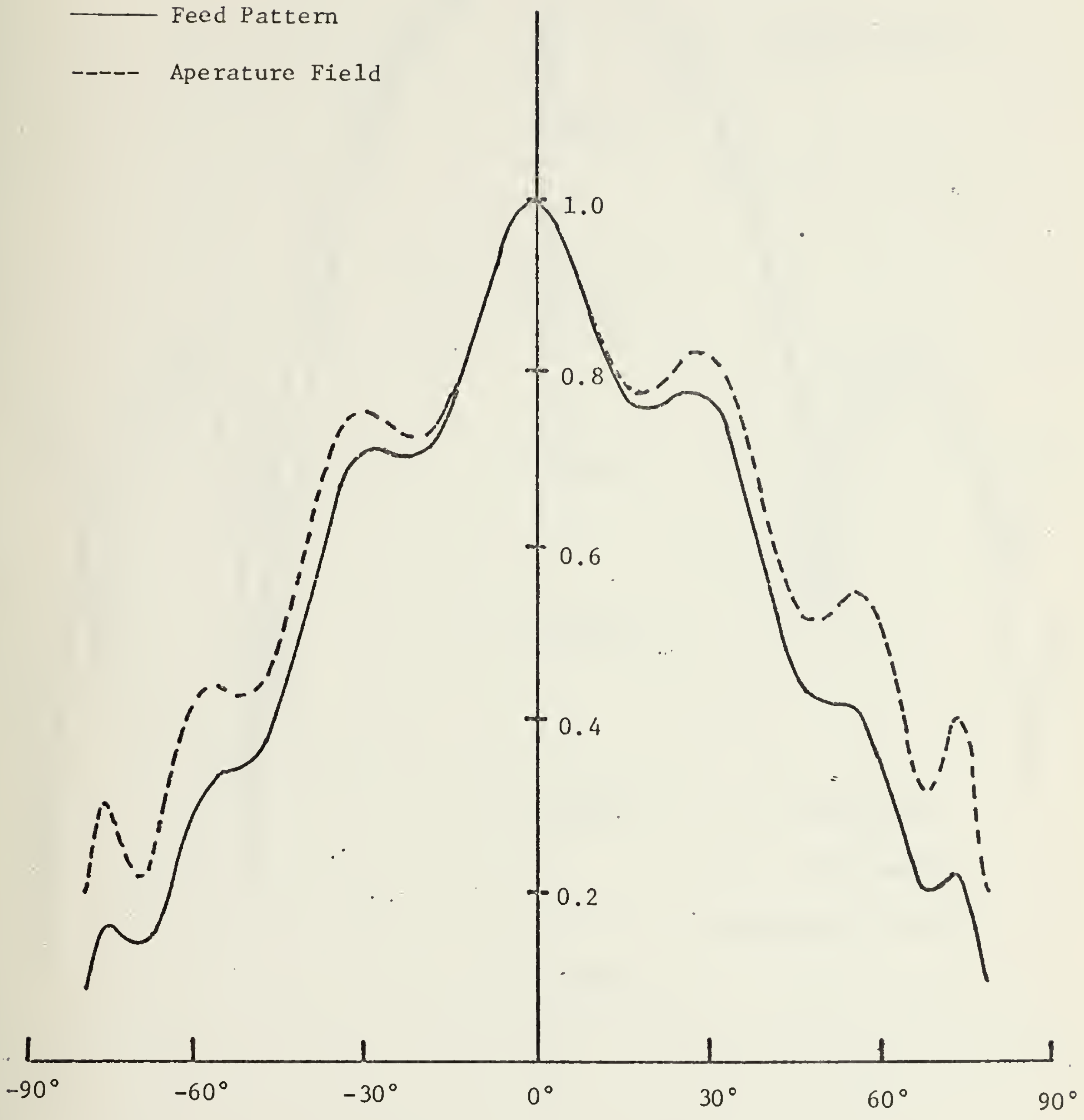

Figure 8. Waveguide Feed Pattern and Luneberg Lens Aperature Field.

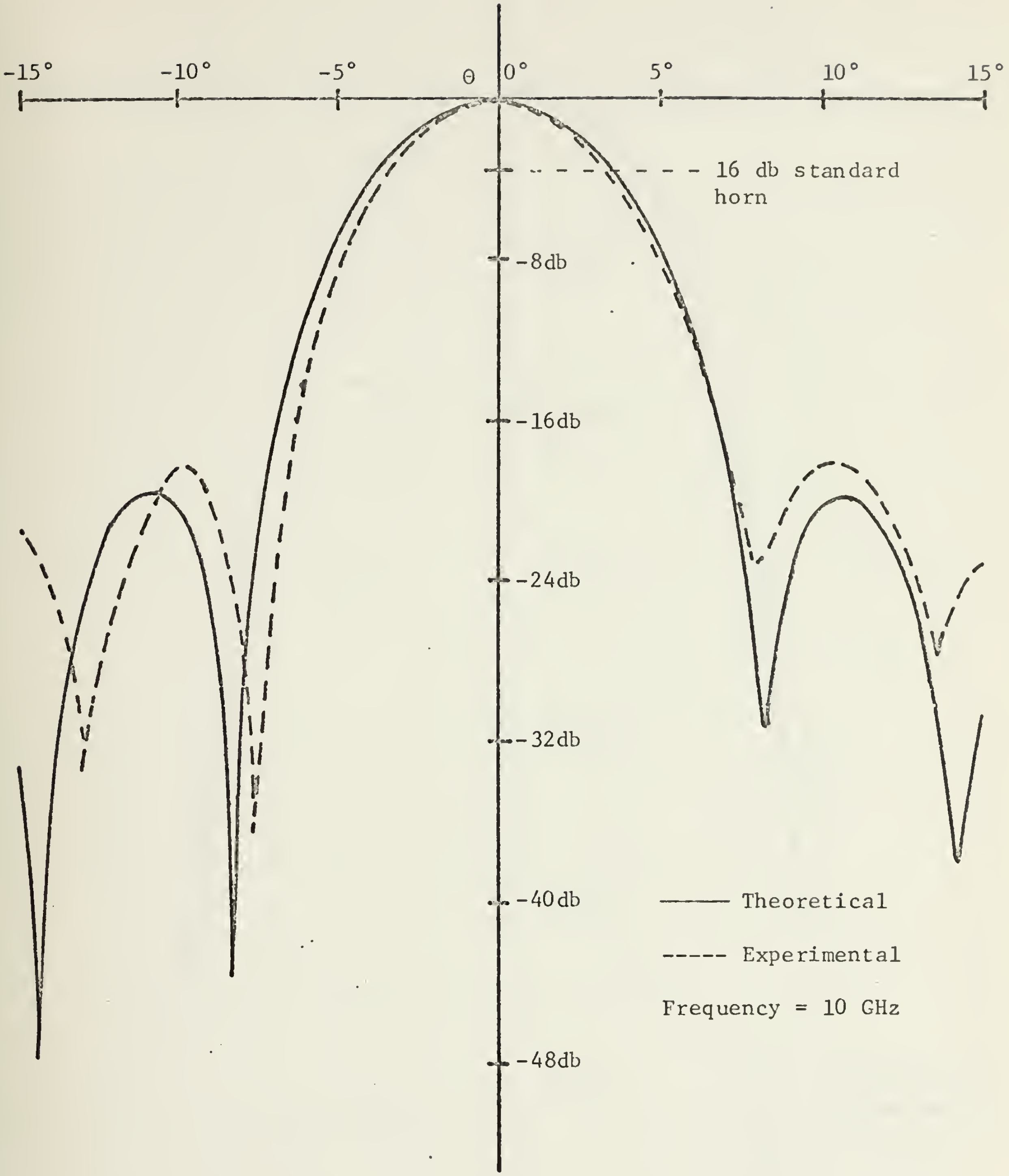

Figure 9. Luneberg Lens Far Field Radiation Patterns with Waveguide Feed.

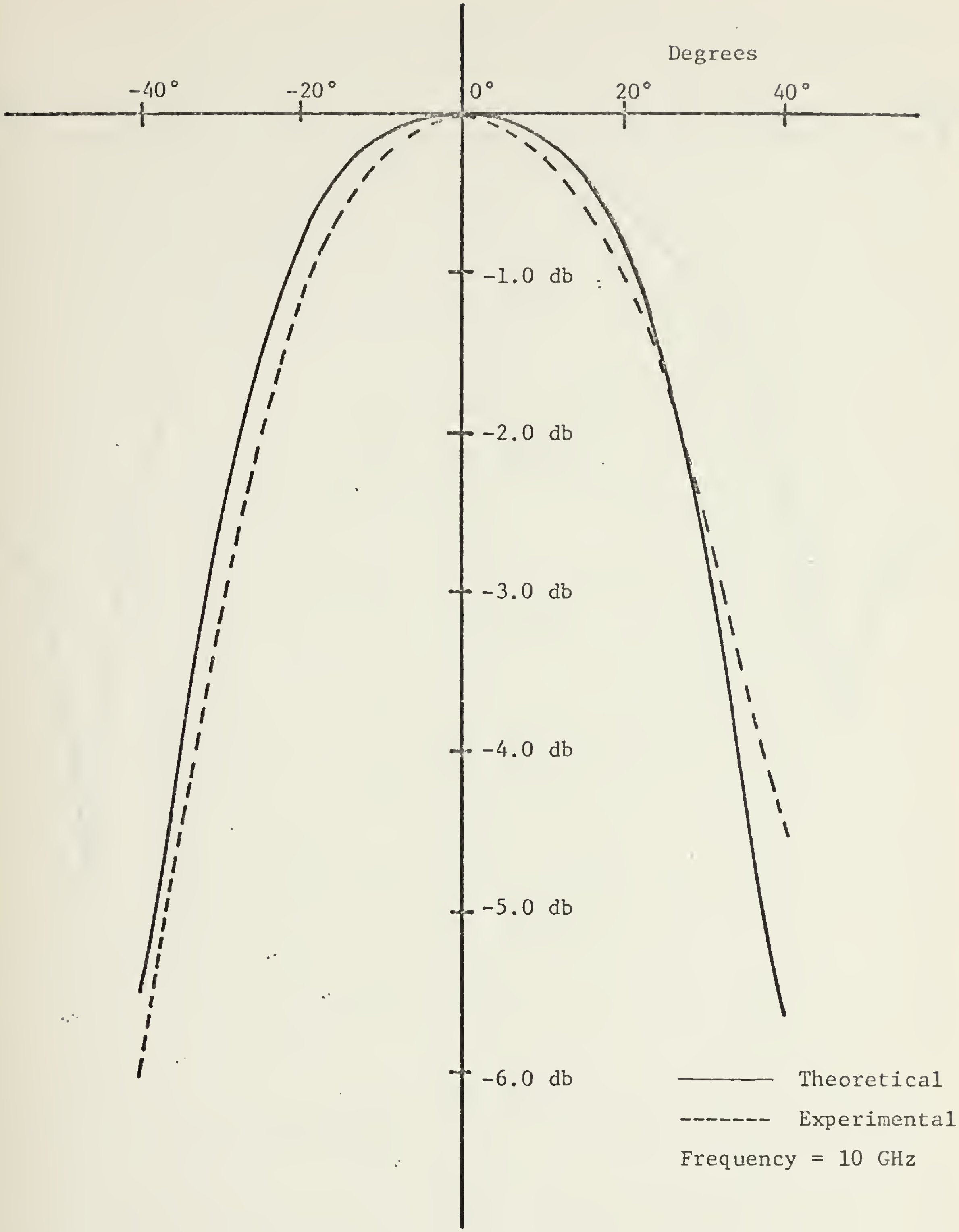

Figure 10. Luneberg Lens (TE_{10} mode) H-plane Far Field Patterns for Waveguide Feed.

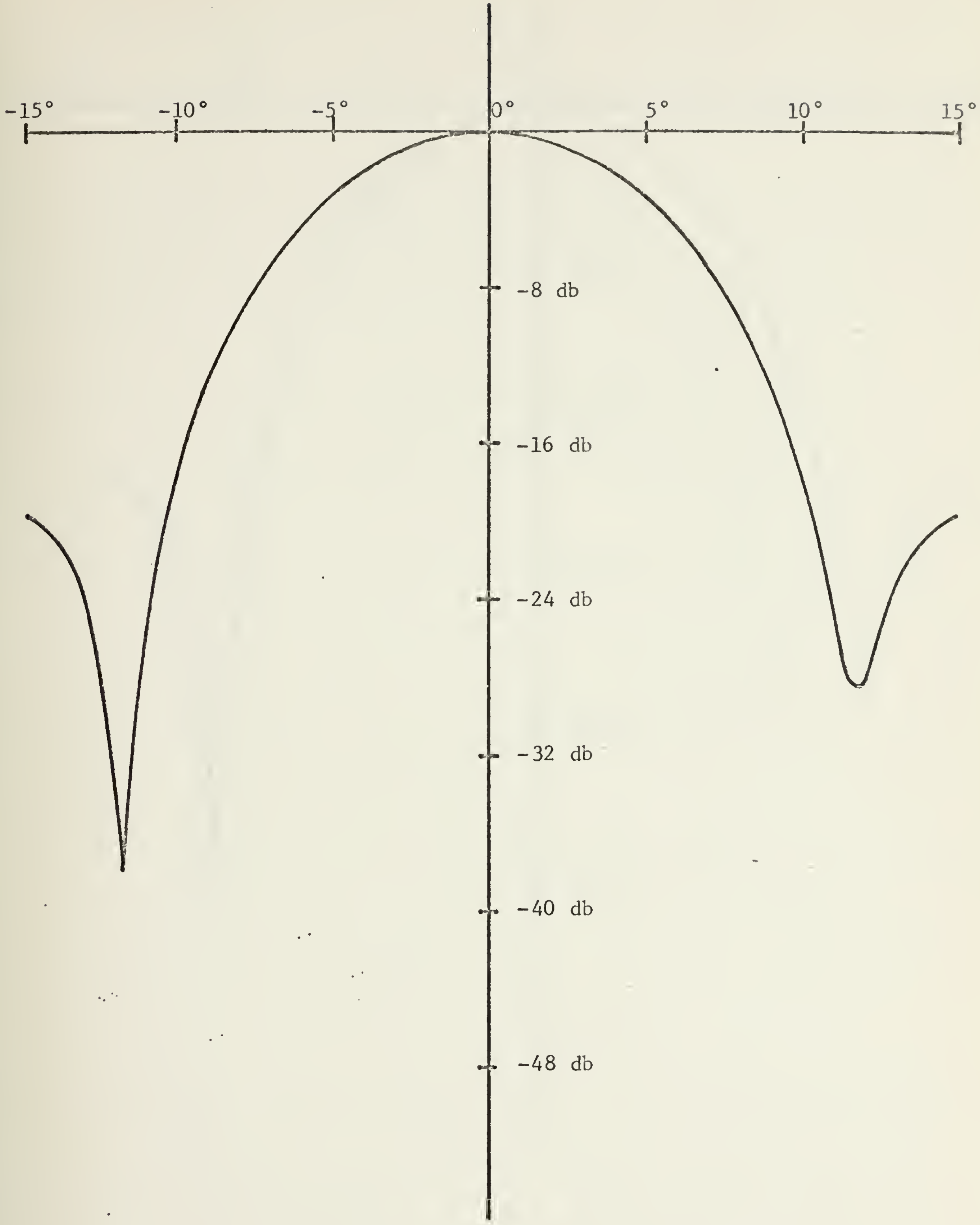

Figure 11. Luneberg Lens E-Plane Patterns for Waveguide Feed at 7.0 GHz.

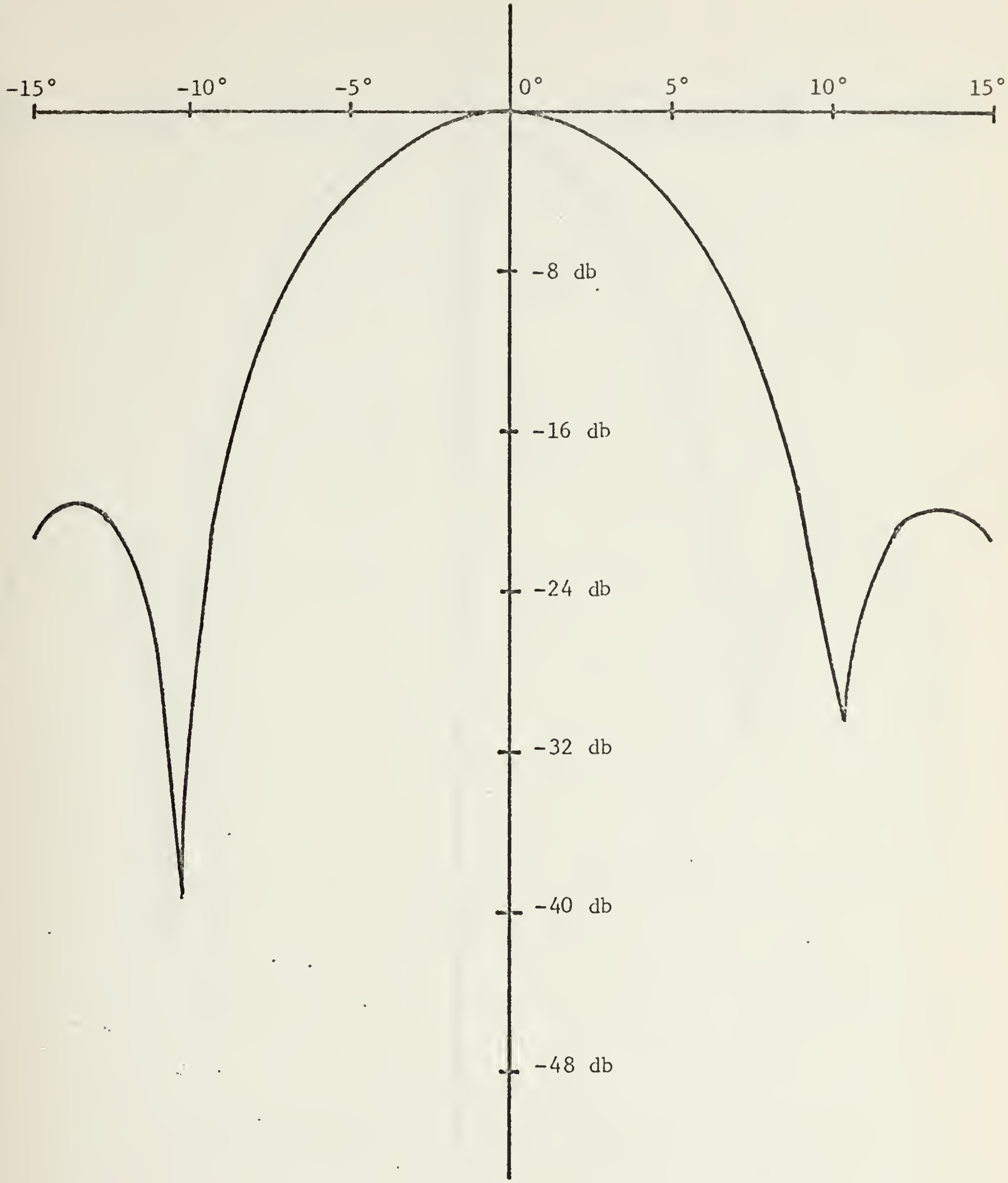

Figure 12. Luneberg Lens E-Plane Patterns for Waveguide Feed at 8.0 GHz.

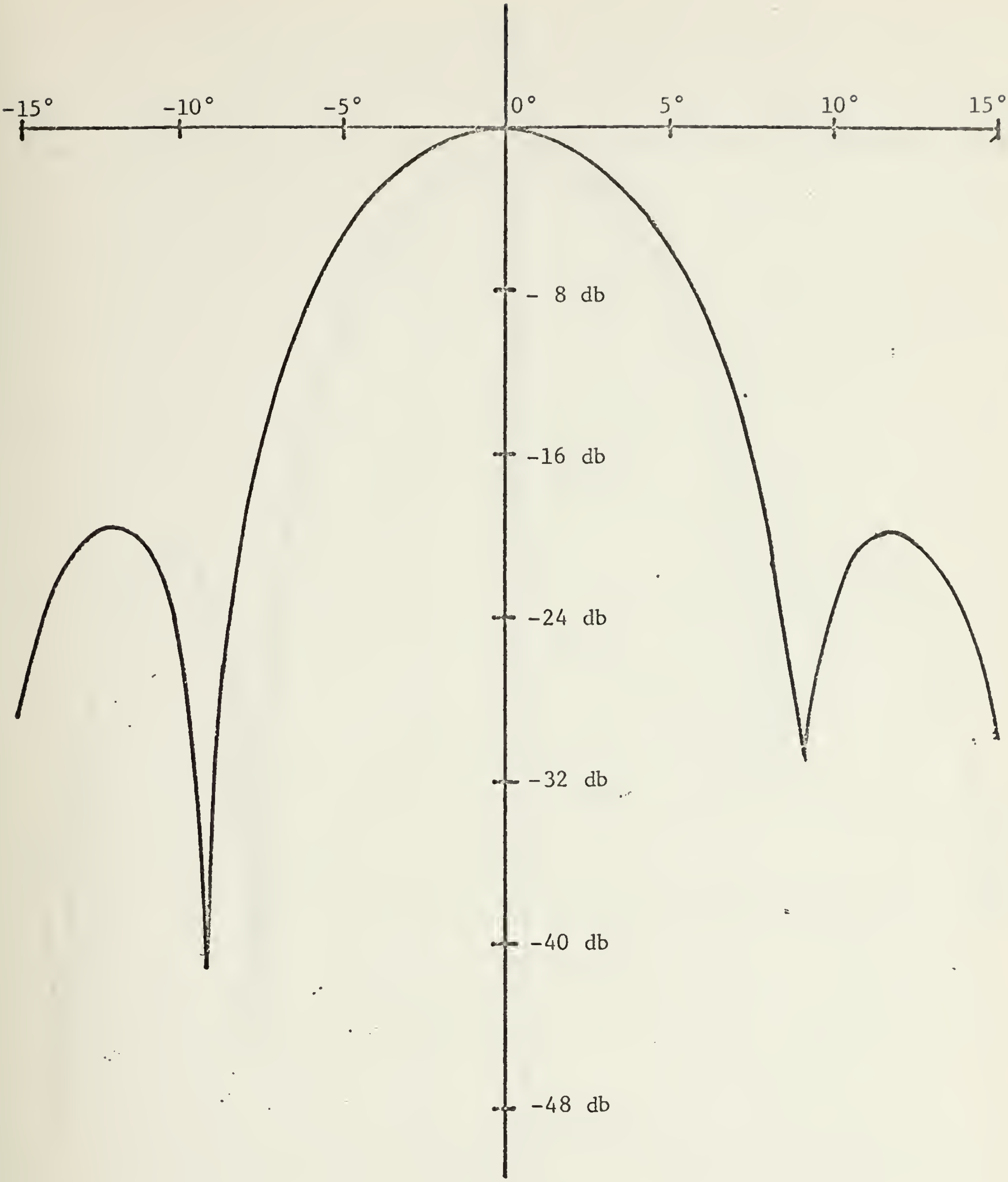

Figure 13. Luneberg Lens E-Plane Patterns for Waveguide Feed at 9.0 GHz.

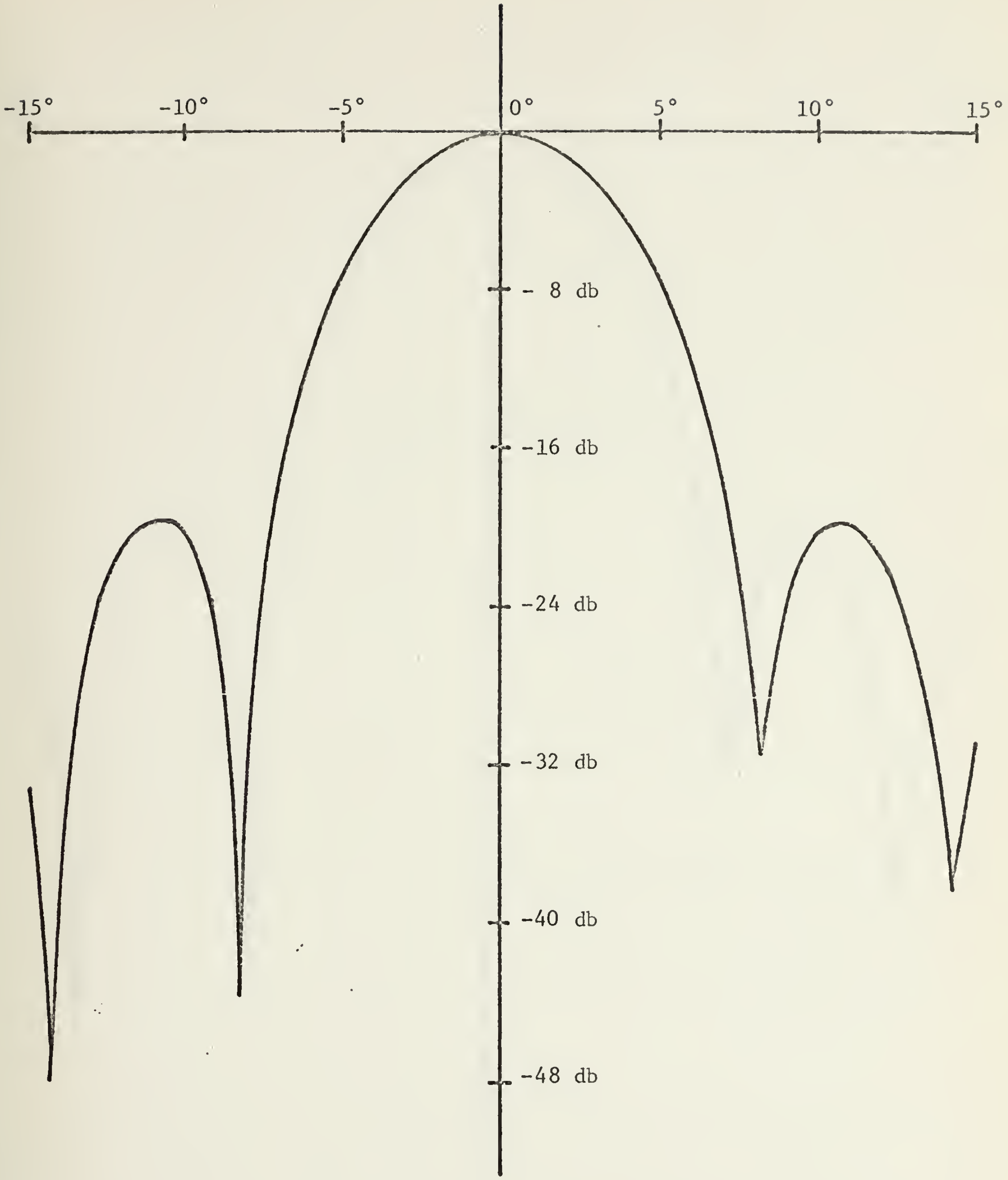

Figure 14. Luneberg Lens E-Plane Patterns for Waveguide Feed at 10 GHz.

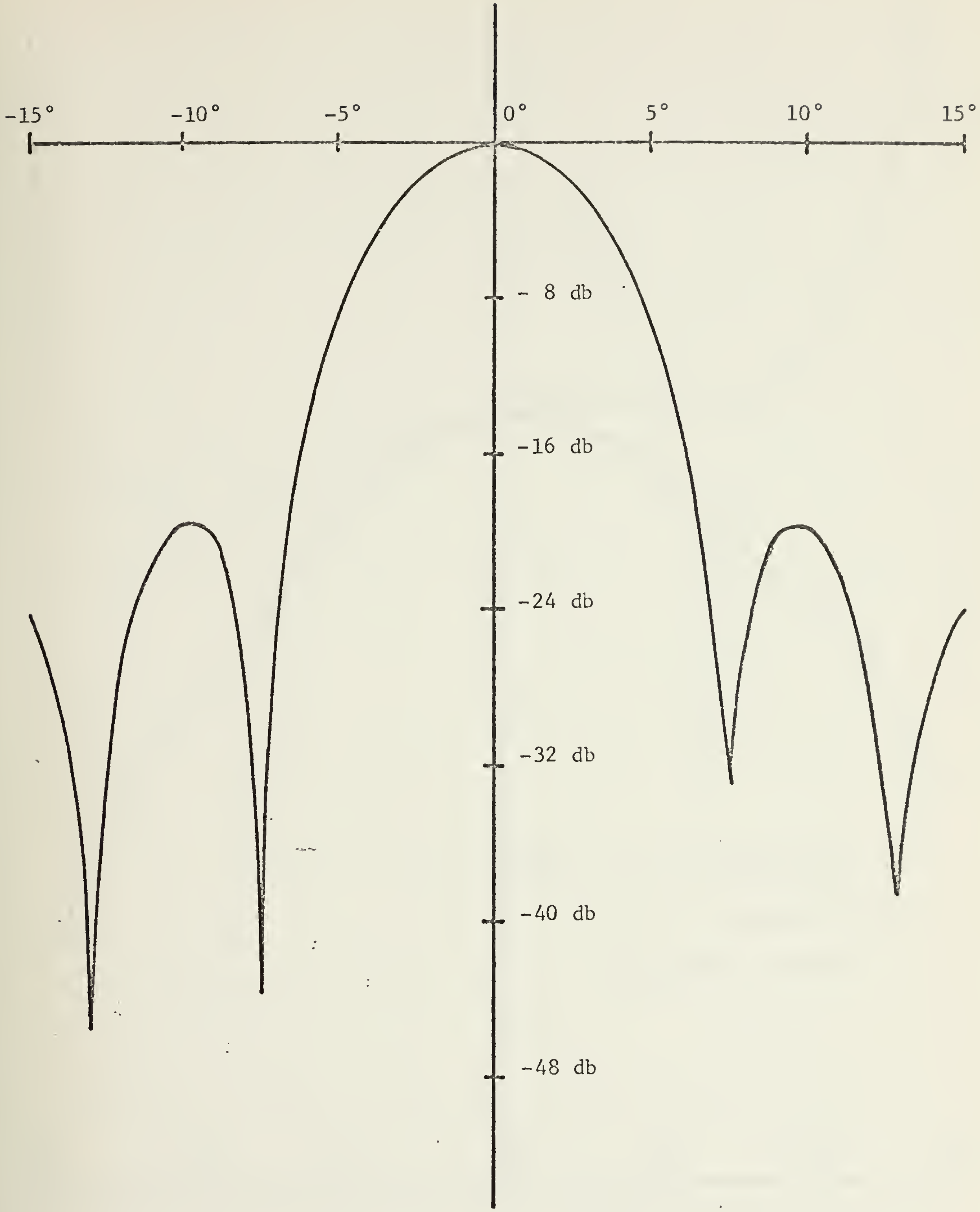

Figure 15. Luneberg Lens E-Plane Patterns for Waveguide Feed at 11 GHz.

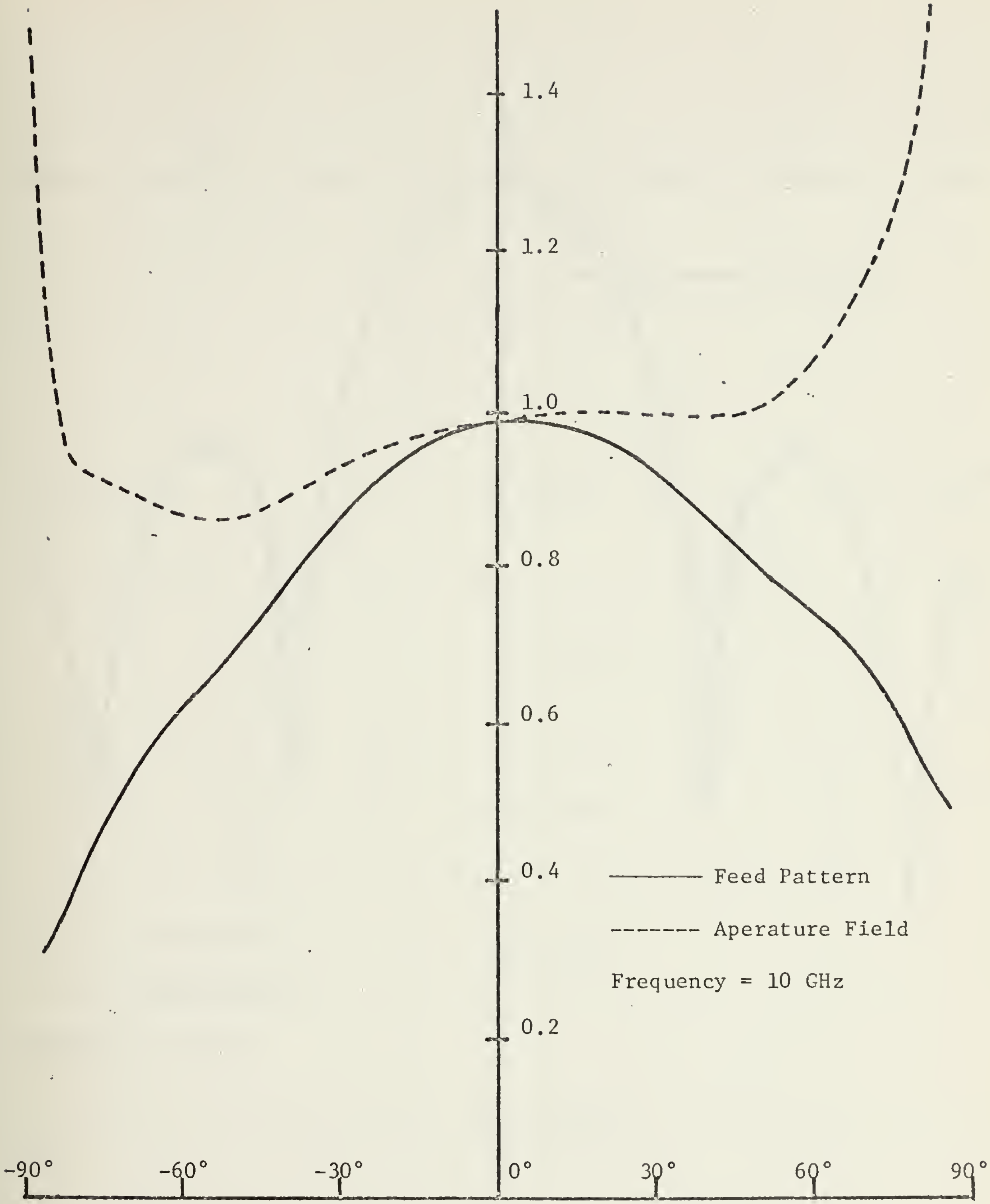

Figure 16. Yagi Array Feed Pattern and Luneberg Lens Aperature Field for Yagi Feed.

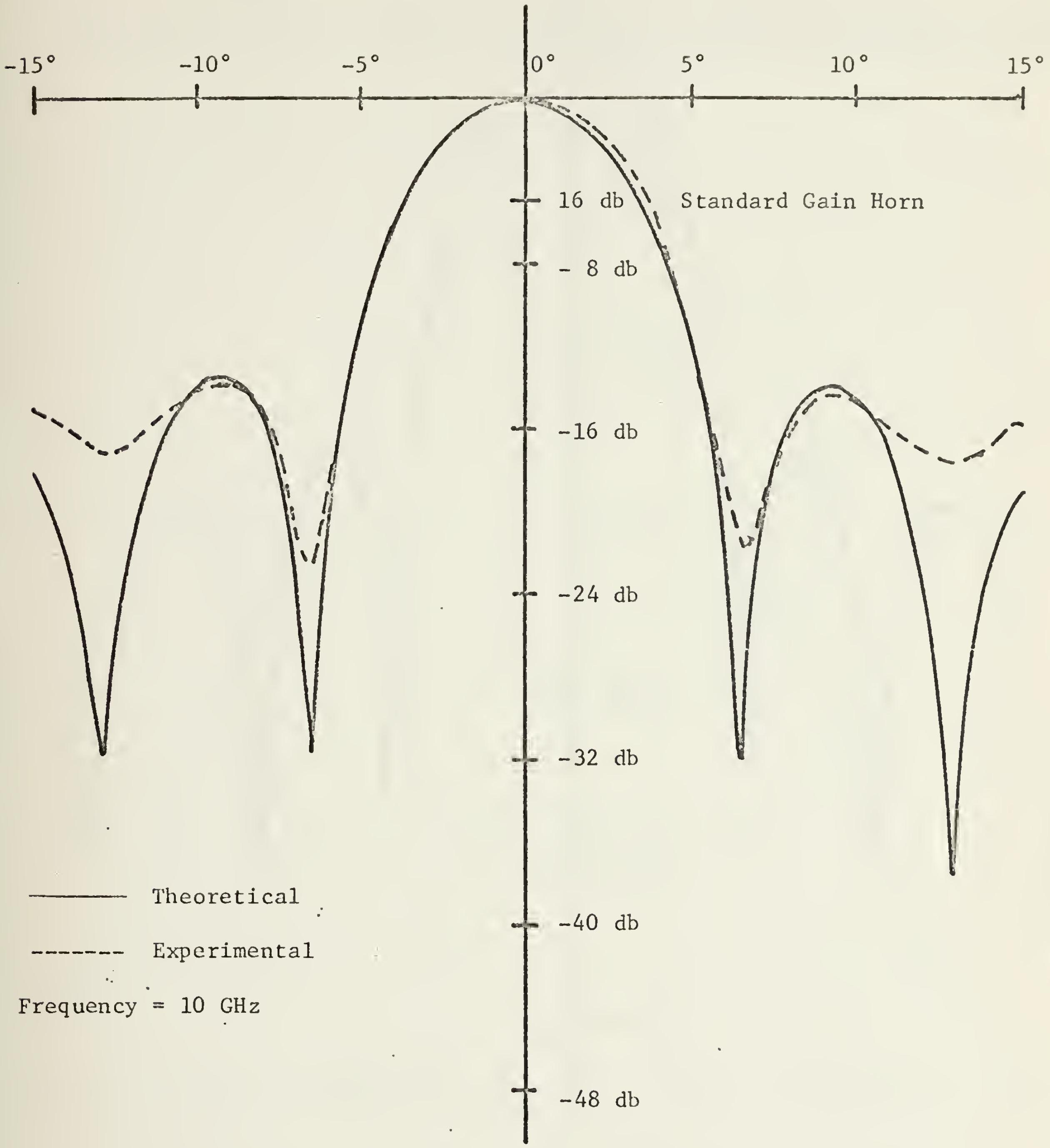

Figure 17. Luneberg Lens (TE_{10} mode) E-Plane Patterns For Yagi Feed at 10 GHz.

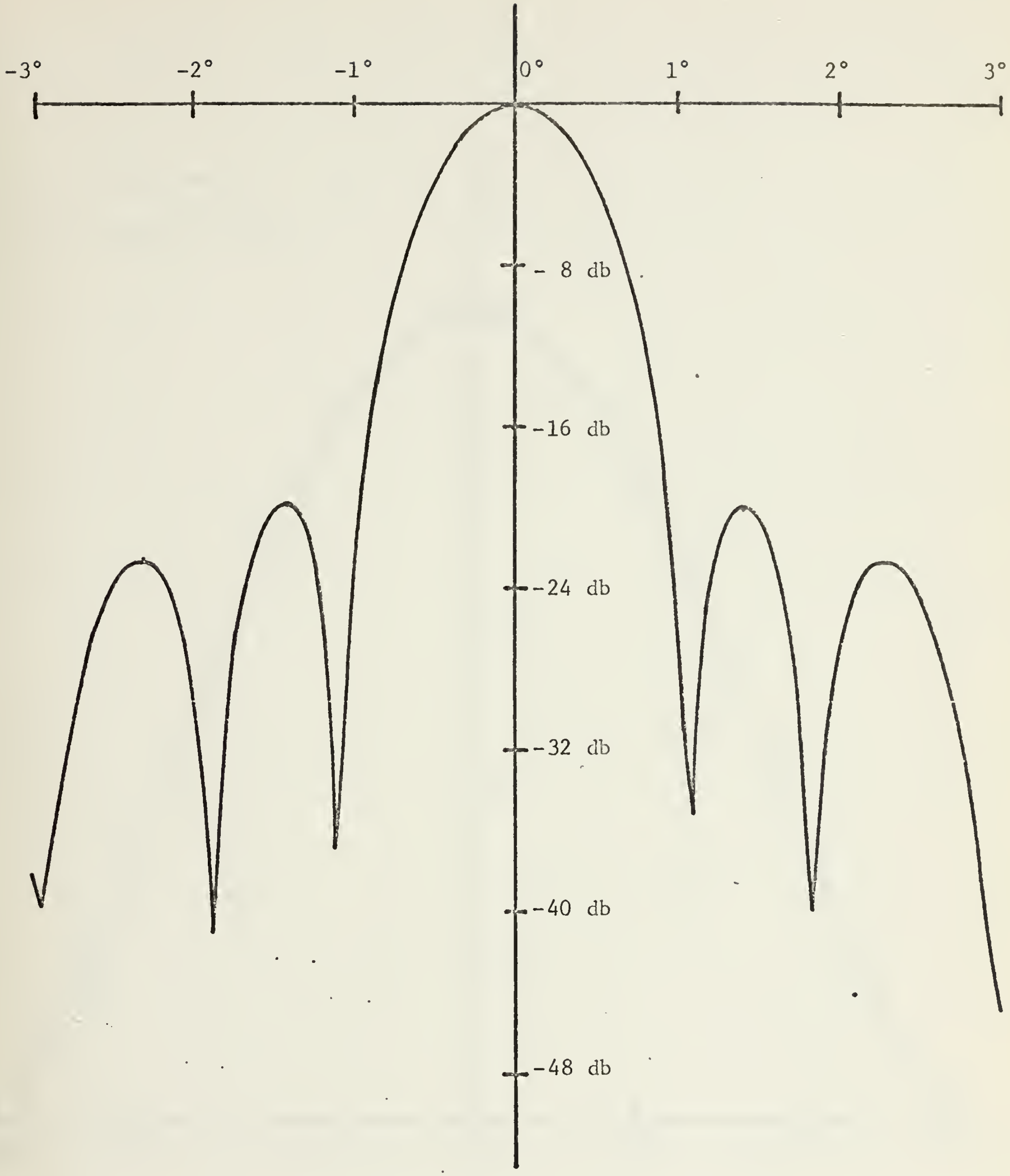

Figure 18. TEM Mode Luneberg Lens Theoretical E-Plane Radiation Patterns With Waveguide Feed at 10 GHz.

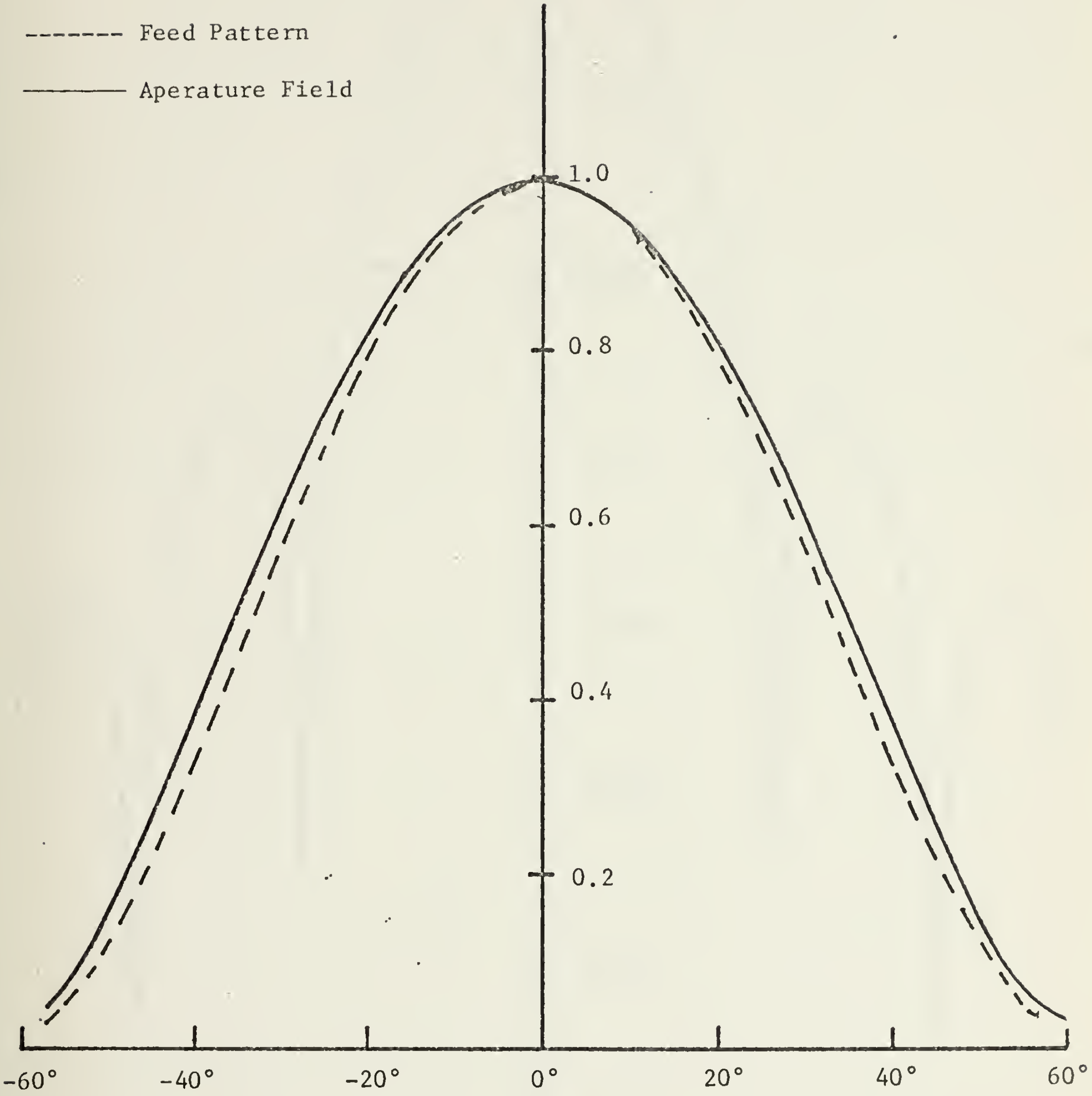

Figure 19. Dielectric Loaded Sectoral Horn Feed Patterns and Aperature Field for Sectoral Horn Feed.

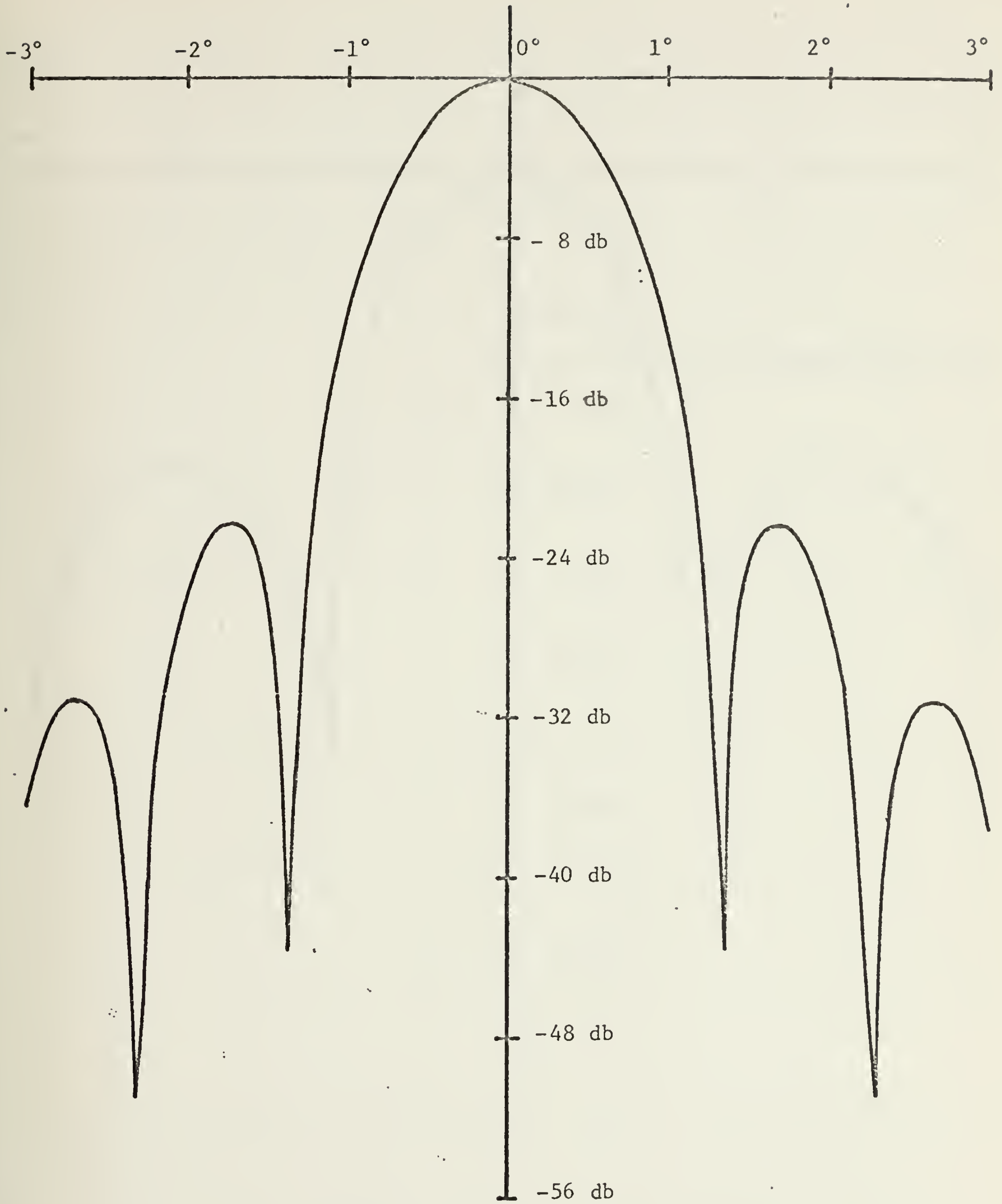

Figure 20. TEM Mode Luneberg Lens Theoretical E-Plane Radiation Patterns For Sectoral Horn Feed at 10 GHz.

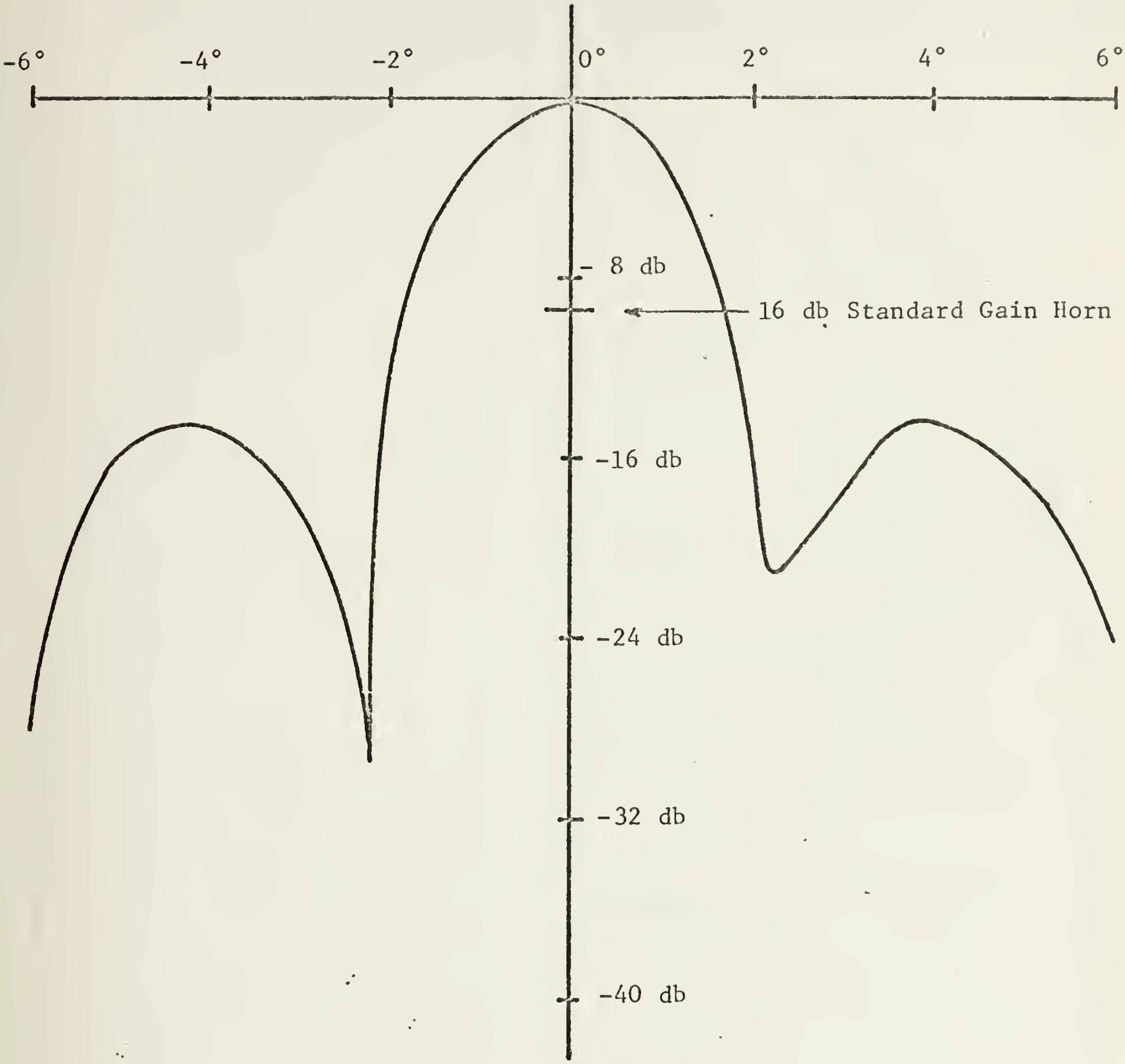

Figure 21. TEM Mode Luneberg Lens Experimental E-Plane Pattern for Sectoral Horn Feed at 10 GHz.

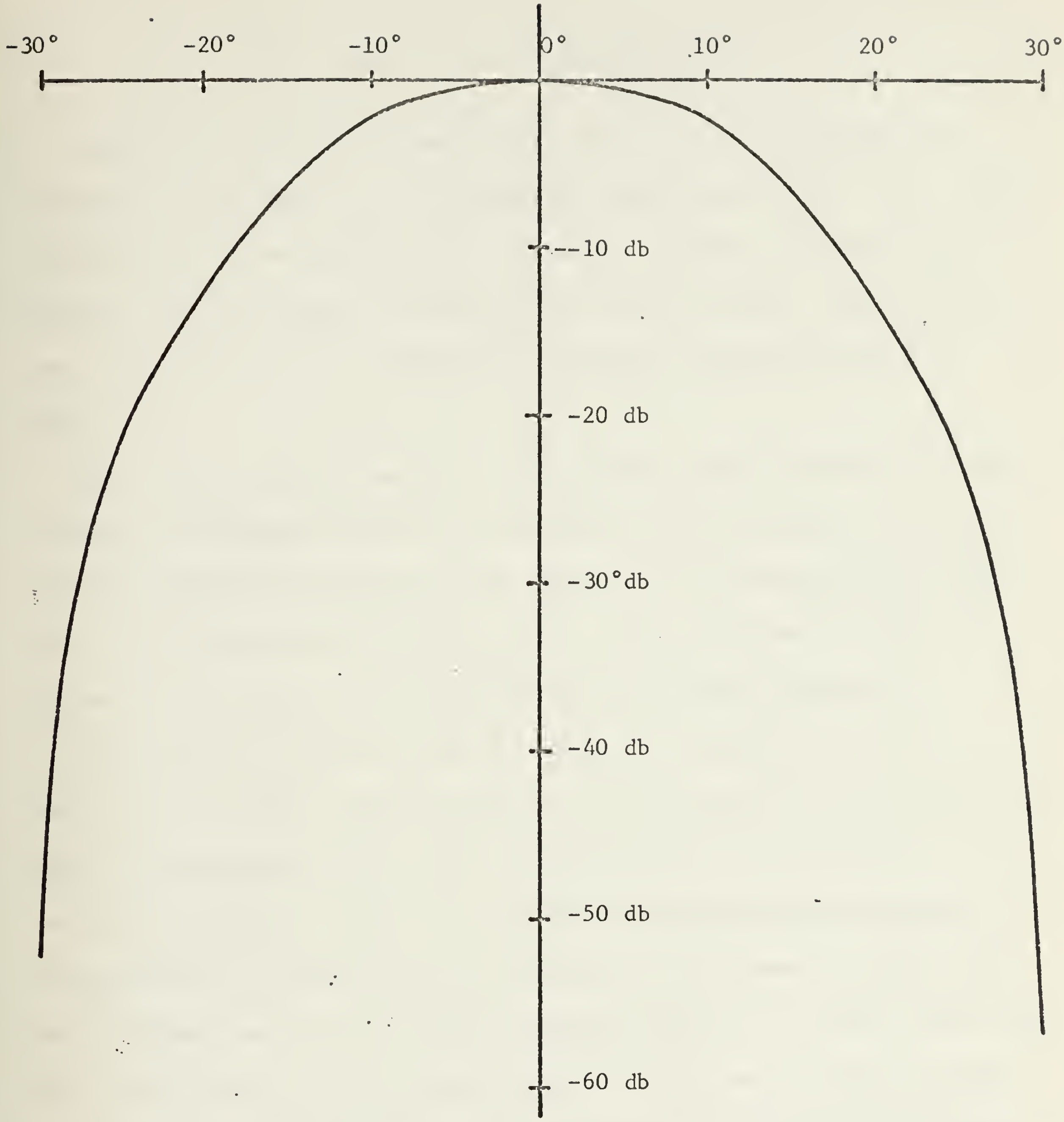

Figure 22. TEM Mode Luneberg Lens H-Plane Radiation Patterns for Sectoral Horn Feed at 10 GHz.

IV. CONCLUSIONS AND RECOMMENDATIONS

The results of the experimentation did not show conclusively the approach of this thesis to the problem of predicting the far field radiation patterns of the Luneberg Lens is valid. However, the results did indicate that the method is valid for the TE_{10} mode lens. There are at least two reasons for the differences, assuming that the approach is valid.

First, the far field patterns of the feed systems were used in calculating the aperature fields and far-field patterns of the lens, when in fact, the lens was not in the far field of the feeds except for the case of the Yagi array on the TE_{10} lens. This resulted in errors in the aperature fields used in calculating the far field patterns.

The results of the TE_{10} mode lens seems to confirm that this was in fact one of the major sources of error. The far field of the waveguide feed is approximately 4 cm. and it was operated at 1.7 cm from the lens for optimum side lobe levels. The differences between the theoretical and experimental patterns were an average of 0.6 degrees in first sidelobe placement and 1.5 db in first sidelobe amplitude. However, when the Yagi array feed, with a far field distance of 0.4 cm., was used at a distance of 1.7 cm from the lens, the differences in first sidelobe placement and amplitude were negligible.

The far field of the dielectric loaded sectoral horn is approximately 9.6 cm. It was operated at about 2 cm from the TEM mode lens and the results were different by about 8 db in the first sidelobe levels and 2.0 degrees in the first sidelobe placement. When the TEM mode lens was fed with the waveguide feed the first sidelobe differences were on

the order of 4.0 db in amplitude and 1.0 degrees in placement. The far field patterns of the TEM mode lens with the waveguide feed were not presented in section III due to the lack of confidence in the results.

Second, the assumption was made that the energy distribution over the x-dimension of the TEM mode lens is constant, while in fact it cannot be due to the metal plates at the top and bottom of the lens. An attempt to measure the aperature field distribution over the x-dimension of the lens failed due to the disturbance of the field caused by the dipole probe used. The x-variation of the aperature field did, however, appear to be a standing wave between the two metal plates.

It is the opinion of the author that the approach of this thesis to the far field analysis of the Luneberg Lens is valid, and that the differences between the theoretical and experimental results is almost completely due to the feed pattern information used in calculating the theoretical patterns.

In line with the above thoughts the following recommendations for future investigations are made:

A. That the near field (theoretical or experimental) of the feeds be used in the calculation of the far field radiation patterns of the Luneberg Lenses.

B. That a broad-band Yagi array, such as Yagi constructed from capacitative lumped loaded cylindrical elements, be used to feed the Luneberg Lens.

C. That multiple Yagi arrays be used to determine the possibility of using electronically scanned Yagi array (such as in item B) to feed the Luneberg Lens in a direction finding system.

D. That the computer programs of Appendix C be modified to calculate the far field patterns of the Constant-K Lens. This would require a change of function subprograms CFCT 3 and CFCT 4 to reflect the geometric optics of the Constant-K Lens.

APPENDIX A

RAY PATH CALCULATIONS

A. DERIVATION OF RAY PATH FORMULA

The generalized Snell's Law for circular symmetry is given in Ref. 3 as

$$n(R)R \sin \Theta = C_1 \tag{34}$$

when

$n(R)$ = Index of refraction

R = Normalized radius

Θ = Angle between ray path and outward meridian

C_1 = Constant

From the geometry of Figure 23,

$$\sin \Theta = \frac{Rd\Psi}{\sqrt{(Rd\Psi)^2 + (dR)^2}} = \frac{R}{\sqrt{R^2 + (\frac{dR}{d\Psi})^2}} \tag{35}$$

Substituting equation (35) into (34) yields

$$C_1 = \frac{nR^2}{\sqrt{R^2 + (\frac{dR}{d\Psi})^2}} \quad \text{or} \quad d\Psi = \frac{C_1 dR}{R\sqrt{n^2R^2 - C_1^2}} . \tag{36}$$

For the Luneberg Lens (normalized radius),

$$n = \sqrt{2 - R^2} \tag{37}$$

which yields

$$d\Psi = \frac{C_1 dR}{R\sqrt{-R^4 + 2R^2 - C_1^2}} \tag{38}$$

or

$$\Psi = C_1 \int \frac{1}{R}[-R^4 + 2R^2 - C_1^2]^{-1/2} dR. \tag{39}$$

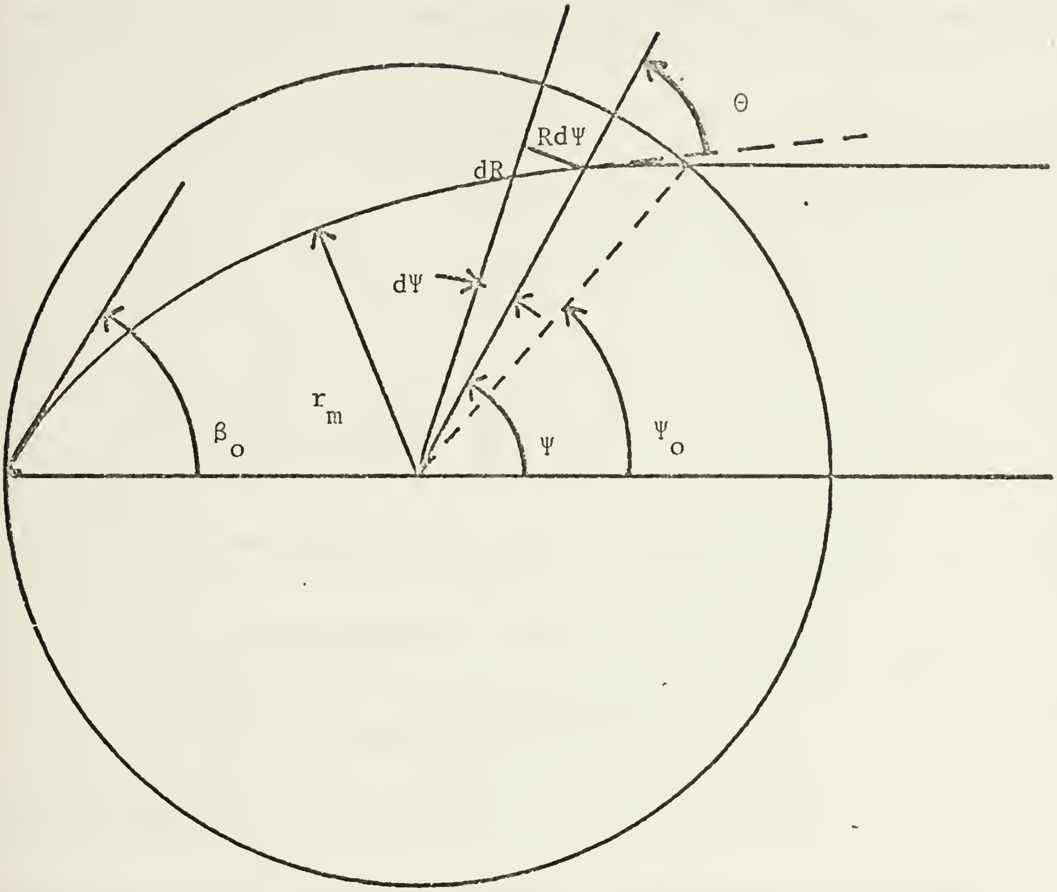
Θ
RdΨ
dR
dΨ
r_m
β_o
Ψ
Ψ_o

Figure 23. Geometry For Luneberg Lens Ray Path Derivations.

Integrating this equation

$$\Psi = \frac{1}{2}\sin^{-1}\sqrt{1-C_1^2} - \frac{1}{2}\sin^{-1}[(R^2-C_1^2)/(R^2\sqrt{1-C_1^2})]. \qquad (40)$$

This equation gives four values of Ψ for each value of C_1 and R and hence two rays. Geometrical considerations produce the following formulas:

$$\Psi_1 = \frac{\pi}{2} - \sin^{-1}\sqrt{1-C_1^2} + \Psi \qquad (41)$$

and

$$\Psi_2 = \pi - \Psi , \qquad (42)$$

where

$$\Psi = \int_1^R \frac{C_1}{R\sqrt{-R^4 + 2R^2 - C_1^2}} dR ,$$

Ψ_1 corresponds to Ψ for $\Psi_m \leq \Psi \leq \pi$,

Ψ_2 corresponds to Ψ for $\Psi_o < \Psi < \Psi_m$,

and Ψ_m is the value of Ψ for which $R = r_m$.

B. CALCULATIONS OF r_m.

For each ray path the closest point of approach to the origin, r_m, occurs for $\Theta = 90°$. Therefore, from equations (34) and (37)

$$r_m[n(r_m)] \sin 90° = C_1,$$

or

$$r_m\sqrt{2-r_m^2} = C_1.$$

Squaring both sides yields

$$r_m^4 - 2r_m^2 + C_1^2 = 0$$

or, by the quadratic formula,

$$r_m = 1 \pm \sqrt{1-C_1^{\,2}} \ .$$

The negative square root must be taken since the positive square root gives an r_m greater than the normalized radius. Therefore,

$$r_m = (1 - \sqrt{1-C_1^{\,2}})^{\,1/2} \ , \qquad (43)$$

which is the closest point of approach of the ray path to the center of the lens.

APPENDIX B

ELECTROMAGNETIC FIELD DERIVATION

A. DERIVATION OF ELECTRIC FIELD EQUATIONS.

The field equations for any aperature on which the electric and magnetic currents are known can be calculated utilizing the Aperature Field method and Huygen's Principle as developed in chapter 2 of Ref. 5. The electromagnetic field equations for any aperature [Ref. 5], and the geometry of Figure 24 are:

$$\overline{E} = -\frac{1}{\varepsilon}\overline{\nabla} \times \overline{F} - \frac{j}{\omega\mu\varepsilon}\overline{\nabla} \times \overline{\nabla} \times \overline{A} \qquad (44)$$

and

$$\overline{H} = \frac{1}{\mu}\overline{\nabla} \times \overline{H} - \frac{j}{\omega\mu\varepsilon}\overline{\nabla} \times \overline{\nabla} \times \overline{F}; \qquad (45)$$

where

$$\overline{A} = \frac{\mu}{4\pi}\iint \frac{\overline{J}(x',\Psi')e^{-jk|R_1|}}{|R_1|} dS' \qquad (46)$$

$$\overline{F} = \frac{\varepsilon}{4\pi}\iint \frac{\overline{K}(x',\Psi')e^{-jk|R_1|}}{|R_1|} dS' \qquad (47)$$

$$\overline{J}(x',\Psi') = \overline{n} \times \overline{H}_a \qquad (48)$$

$$\overline{K}(x',\Psi') = \overline{E} \times \overline{n} \qquad (49)$$

$$k = \frac{2\pi}{\lambda} \qquad (50)$$

$$dS' = \rho\ dx'\ d\Psi' \qquad (51)$$

$$|R_1| = [R^2+(R')^2-2R(x'\cos\Phi\cos\Theta-\rho\sin\Psi'\sin\Theta\sin\Phi+\rho\cos\Psi'\cos\Theta)]^{1/2}, \qquad (52)$$

$$\overline{n} = -\sin\Psi'\overline{a}_y + \cos\Psi'\overline{a}_z \equiv \text{unit normal to aperature.} \qquad (53)$$

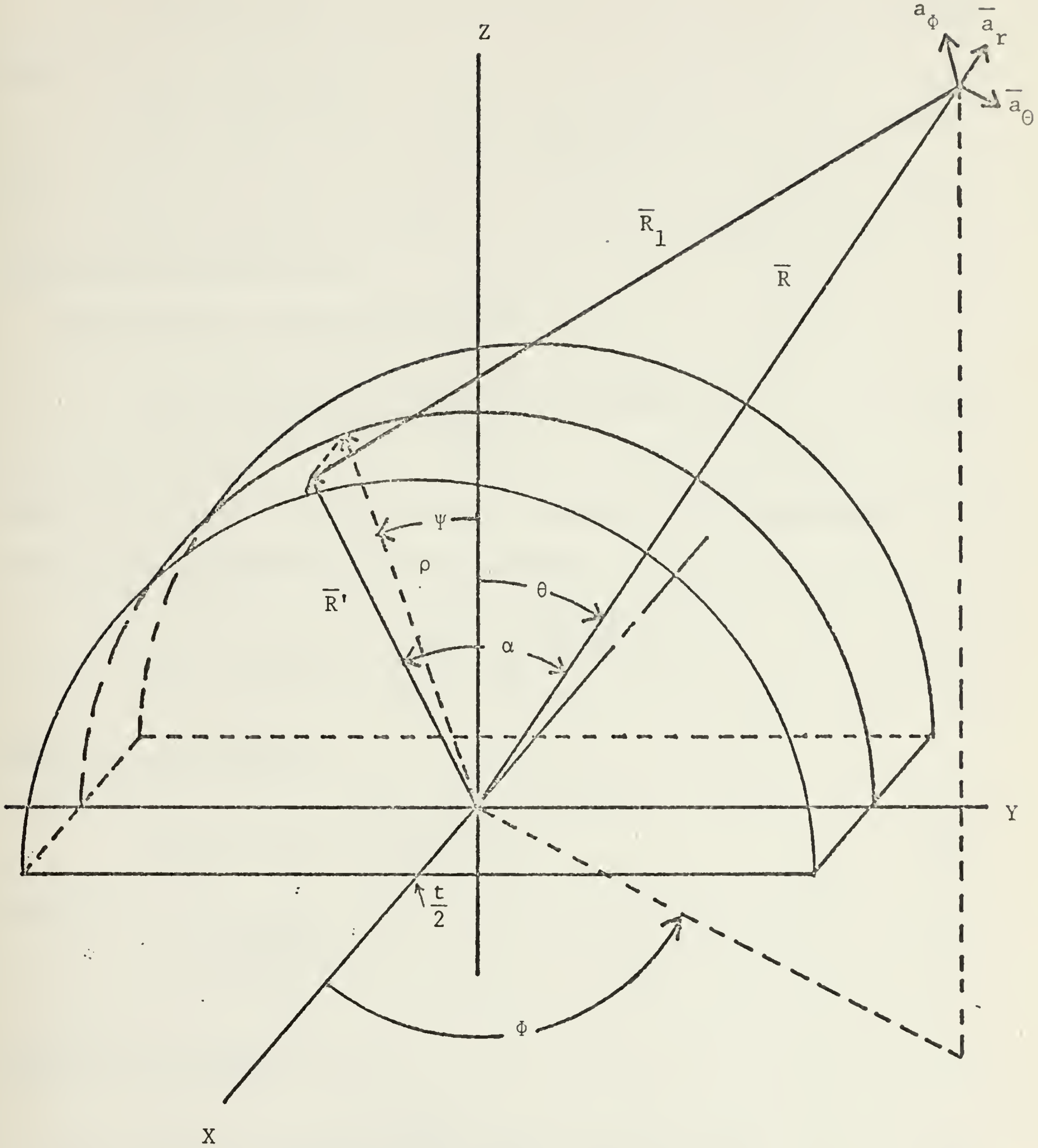
Z
$\bar{a}_\phi$
$\bar{a}_r$
$\bar{a}_\theta$
$\bar{R}_1$
$\bar{R}$
Ψ
ρ
$\bar{R}'$
θ
α
Y
$\frac{t}{2}$
Φ
X

Figure 24. Luneberg Lens Geometry Used in the Derivation of Radiation Expressions.

Equation (1) was divided into two parts:

$$\overline{E} = \overline{E}_1 + \overline{E}_2 \tag{53}$$

where

$$\overline{E}_1 = -\frac{1}{\varepsilon}\overline{\nabla} \times \overline{F} \tag{54}$$

and

$$E_2 = -\frac{j}{\omega\mu\varepsilon}\overline{\nabla} \times \overline{\nabla} \times \overline{A}, \tag{55}$$

and considered separately.

From equations (47), (49) and (54)

$$E_1 = -\frac{1}{\varepsilon}\overline{\nabla} \times \left[\frac{\varepsilon}{4\pi}\iint \frac{\overline{K}(x',\Psi')}{|R_1|} e^{-jk|R_1|} dS'\right]. \tag{56}$$

Taking all constants outside the curl equations and interchanging the order of the integration and curl operators,

$$E_1 = -\frac{1}{4\pi}\iint \overline{\nabla} \times \left[\frac{\overline{K}(x',\Psi')e^{-jk|R_1|}}{|R_1|}\right] dS'. \tag{57}$$

Using the vector identity

$$\overline{\nabla} \times \overline{K}f = \overline{\nabla f} \times \overline{K} + f(\overline{\nabla} \times \overline{K}) \tag{58}$$

where

$$f = \frac{e^{-jk|R_1|}}{|R_1|} \quad , \tag{59}$$

equation (57) reduces to

$$\overline{E}_1 = \frac{1}{4\pi}\iint (jk + \frac{1}{|R_1|})(\frac{e^{-jk|R_1|}}{|R_1|})(\overline{a}_r \times \overline{K}(x',\Psi'))\ dS' \ , \tag{60}$$

since

$$\overline{\nabla f} = (\frac{-jk}{|R_1|} - \frac{1}{|R_1|^2})e^{-jk|R_1|}$$

and $\overline{\nabla} \times \overline{K} = 0.$[4]

---

[4] $\overline{K}$ is independent of the point of observation.

From equations (46) and (55)

$$E_2 = \frac{-j}{\omega\mu\varepsilon}\,\bar{\nabla}\times\bar{\nabla}\times\left[\frac{\mu}{4\pi}\iint\frac{\bar{J}(x',\psi')e^{-jk|R_1|}}{|R_1|}\,ds'\right].$$

Taking all constants outside the curl equations and interchanging the order of integration and the curl operators

$$E_2 = \frac{-j}{4\pi\omega\varepsilon}\iint\bar{\nabla}\times\bar{\nabla}\times\left[\frac{\bar{J}(x',\psi')e^{-jk|R_1|}}{|R_1|}\right]dS'. \tag{61}$$

Applying the vector identity of equation (58) to the integrand twice yields

$$\bar{\nabla}\times\bar{\nabla}\times\left(\frac{J(x',\psi')e^{-jk|R_1|}}{|R_1|}\right) = \left(-\frac{k^2}{|R_1|}+\frac{2jk}{|R_1|^2}+\frac{2}{|R_1|^3}\right)e^{-jk|R_1|}[\bar{a}_r\times(\bar{a}_r\times\bar{J})] \tag{62}$$

Then from equations (61) and (62)

$$E_2 = \frac{j}{4\pi\omega\varepsilon}\iint\left(k^2-\frac{2jk}{|R_1|}-\frac{2}{|R_1|^2}\right)\left(\frac{e^{-jk|R_1|}}{|R_1|}\right)[\bar{a}_r\times(\bar{a}_r\times\bar{J})]\,ds'. \tag{63}$$

Equations (51), (53), (60) and (63) yield the Electric Field or any cylindrical aperature field at any distance from the aperature. For the far field only, the $1/|R_1|^2$ and $1/|R_1|^3$ terms can be neglected leaving

$$E_1 = \frac{jk\rho}{4\pi}\iint\frac{e^{-jk|R_1|}}{|R_1|}(\bar{a}_r\times\bar{K}(x',\Psi'))dx'\,d\Psi'. \tag{64}$$

and

$$E_2 = \frac{jk^2\rho}{4\pi\omega\varepsilon}\iint\frac{e^{-jk|R_1|}}{|R_1|}[\bar{a}_r\times(\bar{a}_r\times\bar{J}(x',\Psi')]dx'\,d\Psi'. \tag{65}$$

The Luneberg Lens was designed to produce constant phase along a line perpendicular to the aperature center and therefore the aperature field

has a phase of $k\rho(1 - \cos\Psi')$ so that:

$$\overline{E}_a = \overline{E}_{a_1} e^{jk\rho(1 - \cos \Psi')}$$

and

$$\overline{H}_a = \overline{H}_{a_1} e^{jk\rho(1 - \cos \Psi')}$$

$\overline{E}_{a_1}$ and $\overline{H}_{a_1}$ are the E and H fields of the aperature.

$\overline{K}$ and $\overline{J}$ can then be rewritten as

$$\overline{K} = (\overline{E}_{a_1} \times \overline{n})e^{jk\rho(1 - \cos \Psi')} = \overline{K}_1 e^{jk\rho(1 - \cos \Psi')} \tag{66}$$

and

$$\overline{J} = (\overline{n} \times \overline{H}_{a_1})e^{jk\rho(1 - \cos \Psi')} = \overline{J}_1 e^{jk\rho(1 - \cos \Psi')} \tag{67}$$

Equations (64) and (65) can be rewritten as

$$\overline{E}_1 = \frac{jk\rho}{4\pi} \iint \frac{e^{-jk|R_1|} e^{jk\rho(1 - \cos \Psi')}}{|R_1|} \overline{F}_1 \, dx' \, d\Psi' \tag{68}$$

and

$$\overline{E}_2 = \frac{jk^2\rho}{4\pi\omega\varepsilon} \iint \left(\frac{e^{-jk|R_1|} e^{jk\rho(1 - \cos \Psi')}}{|R_1|}\right)\overline{F}_2 \, dx' \, d\Psi' \tag{69}$$

where

$$\overline{F}_1 = \overline{a}_r \times \overline{K}(x',\psi') = \overline{a}_r \times (\overline{E}_{a_1} \times \overline{n}), \tag{70}$$

and

$$\overline{F}_2 = \overline{a}_r \times (\overline{a}_r \times \overline{J}_1(x',\Psi') = \overline{a}_r \times [\overline{a}_r \times (\overline{n} \times \overline{H}_{a_1})] \tag{71}$$

From equation (70) and vector identity

$$\overline{A} \times (\overline{B} \times \overline{C}) = (\overline{A} \cdot \overline{C})\overline{B} - (\overline{A} \cdot \overline{B})\overline{C}, \tag{72}$$

$$\overline{F}_1 = (\overline{a}_r \cdot \overline{n})\overline{E}_{a_1} - (\overline{a}_r \cdot \overline{E}_{a_1})\overline{n},$$

or

$$\overline{F}_1 = C_7\overline{E}_{a_1} - C_8\overline{n} , \tag{73}$$

where

$$C_7 \equiv \overline{a}_r \cdot \overline{n},$$

and

$$C_8 \quad \bar{a}_r \cdot \bar{E}_{a_1} . \qquad (75)$$

Assuming that the aperature field is polarized in the x-direction (i.e. $\bar{E}_{a_1} = E_{ax}\,\bar{a}_x$ and $\bar{H}_{a_1} = H_{ay}\,\bar{a}_y$)

$$C_7 = - \sin \Theta \sin \Phi \sin \Psi' + \cos \Theta \cos \Psi' \qquad (76)$$

and

$$C_8 = E_{ax} \sin \Theta \cos \Phi . \qquad (77)$$

Combining equations (73), (76) and (77) gives

$$\begin{aligned} \bar{F}_1 &= (-\sin \Theta \sin \Phi \sin \Psi' + \cos \Theta \cos \Psi) E_{ax}\,\bar{a}_x \\ &+ E_{ax} \sin \Theta \cos \Phi \sin \Psi'\,\bar{a}_y \\ &- E_{ax} \sin \Theta \cos \Phi \cos \Psi'\,\bar{a}_z \end{aligned} \qquad (78)$$

Converting to spherical coordinates

$$\bar{F}_1 = F_{1r}\,\bar{a}_r + F_{1\Theta}\,\bar{a}_\Theta + F_{1\Phi}\,\bar{a}_\Phi \qquad (79)$$

where

$$F_{1r} = 0 \quad , \qquad (80)$$

$$F_{1\Theta} = E_{ax} \cos \Psi' \cos \Phi \; , \qquad (81)$$

and

$$F_{1\Phi} = E_{ax} (\sin \Theta \sin \Psi' - \cos \Theta \cos \Psi' \sin \Phi) . \qquad (82)$$

When the above equations are substituted into equation (68)

$$\bar{E} = \frac{jk\rho}{4\pi} \iint \frac{e^{-jk|R_1|} e^{jk\rho(1 - \cos \Psi')}}{|R_1|} [F_{1r}\bar{a}_r + F_{1\Theta}\bar{a}_\Theta + F_{1\Phi}\bar{a}_\Phi] dx'\, d\Psi' \qquad (83)$$

or

$$\bar{E}_1 + E_{1r}\bar{a}_r + E_{1\Theta}\bar{a}_\Theta + E_{1\Phi}\bar{a}_\Phi \qquad (84)$$

where

$$E_{1r} = 0, \qquad (85)$$

$$E_{1\Phi} = \frac{jk\rho}{4\pi} \iint \frac{e^{-jk|R_1|} e^{jk\rho(1 - \cos \Psi')}}{|R_1|} F_{1\Phi} \, dx' \, d\Psi' \tag{86}$$

and

$$E_{1\Theta} = \frac{jk\rho}{4\pi} \iint \frac{e^{-jk|R_1|} e^{jk\rho(1 - \cos \Psi')}}{|R_1|} F_{1\Theta} \, dx' \, d\Psi' \tag{87}$$

Similarly, from equations (71) and (72)

$$F_2 = \bar{a}_r \times (C_9 \bar{n} - C_7 \bar{H}_a)$$

or

$$F_2 = C_9(\bar{a}_r \times \bar{n}) - C_7(\bar{a}_r \times \bar{H}_a), \tag{88}$$

where

$$C_9 \equiv \bar{a}_r \cdot \bar{H}_a \tag{89}$$

and

$$\begin{aligned} \bar{a}_r \times \bar{n} = {} & (\sin \Theta \sin \Phi \cos \Psi' + \cos \Theta \sin \Psi') \bar{a}_x \\ & - \sin \Theta \cos \Phi \cos \Psi' \, \bar{a}_y \\ & - \sin \Theta \cos \Phi \sin \Psi' \, \bar{a}_z \, . \end{aligned} \tag{90}$$

Again assuming an aperature field polarized in the x-direction

$$\bar{H}_{a_1} = H_{ay} \bar{a}_y \, , \tag{91}$$

$$\bar{a}_r \times \bar{H}_a = - H_{ay} \cos \Theta \, \bar{a}_x + H_{ay} \sin \Theta \cos \Phi \, \bar{a}_z, \tag{92}$$

$$C_9 = H_{ay} \sin \Theta \sin \Phi \, , \tag{93}$$

and C_7 is as given by equation (76). From equations (76) and (88-93)

$$\begin{aligned} \bar{F}_2 = {} & H_{ay}(\sin^2\Theta \sin^2\Phi \cos \Psi' + \cos^2\Theta \cos \Psi')\bar{a}_x \\ & - H_{ay} \sin^2\Theta \sin \Phi \cos \Phi \cos \Psi' \, \bar{a}_y \\ & - H_{ay} \sin \Theta \cos \Phi \cos \Theta \cos \Psi' \, \bar{a}_z . \end{aligned} \tag{94}$$

Converting to spherical coordinates

$$\bar{F}_2 = F_{2r} \bar{a}_r + F_{2\Theta} \bar{a}_\Theta + F_{2\Phi} \bar{a}_\Phi \tag{95}$$

or

$$\overline{E}_2 = \frac{jk^2\rho}{4\pi\omega\varepsilon}\iint \frac{e^{-jk|R_1|}e^{jk\rho(1 - \cos\Psi')}}{|R_1|}(F_{2r}\overline{a}_r + F_{2\Theta}\overline{a}_\Theta + F_{2\Phi}\overline{a}_\Phi)dx'\,d\Psi' \tag{96}$$

where

$$F_{2r} = 0, \tag{97}$$

$$F_{2\Theta} = H_{ay}\cos\Theta\cos\Psi'\cos\Phi\ , \tag{98}$$

and

$$F_{2\Phi} = -H_{ay}\sin\Phi\cos\Psi'. \tag{99}$$

When the above equations are substituted into equation (69)

$$\overline{E}_2 = \frac{jk^2\rho}{4\pi\omega\varepsilon}\iint \left[\frac{e^{-jk|R_1|}e^{jk\rho(1 - \cos\Psi')}}{|R_1|}\right][F_{2r}\overline{a}_r + F_{2\Theta}\overline{a}_\Theta + F_{2\Phi}\overline{a}_\Phi]dx'd\Psi' \tag{100}$$

or

$$\overline{E}_2 = E_{2r}\overline{a}_r + E_{2\Theta}\overline{a}_\Theta + E_{2\Phi}\overline{a}_\Phi; \tag{101}$$

where

$$E_{2r} = 0, \tag{102}$$

$$E_{2\Theta} = \frac{jk^2\rho}{4\pi\omega\varepsilon}\iint \frac{e^{-jk|R_1|}e^{jk\rho(1 - \cos\Psi')}}{|R_1|}F_{2\Theta}\,dx'd\Psi'\ , \tag{103}$$

and

$$E_{2\Phi} = \frac{jk^2\rho}{4\pi\omega\varepsilon}\iint \frac{e^{-jk|R_1|}e^{jk\rho(1 - \cos\Psi')}}{|R_1|}F_{2\Phi}\,dx'd\Psi'. \tag{104}$$

From equation (53)

$$\overline{E} = \overline{E}_1 + \overline{E}_2 = E_r\overline{a}_r + E_\Theta\overline{a}_\Theta + E_\Phi\overline{a}_\Phi \tag{105}$$

where

$$E_r = E_{1r} + E_{2r} \tag{106}$$

$$E_\Theta = E_{1\Theta} + E_{2\Theta}, \tag{107}$$

and

$$E_\Phi = E_{1\Phi} + E_{2\Phi}. \tag{108}$$

Substituting equations (85) and (102) into (106), (87) and (103) into (107), and (86) and (104) into (108),

$$E_r = 0,$$

$$E_\Theta = \frac{jk\rho}{4\pi} \iint [\frac{e^{-jk|R_1|} e^{jk\rho(1 - \cos \Psi')}}{|R_1|}][E_{ax} \cos \Psi' \cos \Phi +$$

$$\frac{k}{\omega\varepsilon} H_{ay} \cos \Theta \cos \Psi' \cos \Phi] \, dx' \, d\Psi' ,$$

and

$$E_\Phi = \frac{jk\rho}{4\pi} \iint [\frac{e^{-jk|R_1|} e^{jk\rho(1 - \cos \Psi')}}{|R_1|}][E_{ax} (\sin \Theta \sin \Psi' -$$

$$- \cos \Theta \cos \Psi' \sin \Phi) + \frac{k}{\omega\varepsilon} H_{ay} \sin \Phi \cos \Psi'] \, dx' \, d\Psi' .$$

Considering the far field relationship of E and H at the aperature of the lens

$$H_{ay} = \sqrt{\frac{\varepsilon}{\mu}} \, \bar{E}_{ax}$$

which when substituted in the above equations yields

$$E_r = 0, \tag{109}$$

$$E_\Theta = \frac{jk\rho}{4\pi} [\cos \Phi \ (1 + \cos \Theta] e^{-jk\rho} \cdot$$

$$\iint \frac{e^{-jk|R_1|} e^{jk\rho \cos \Psi'}}{|R_1|} E_{ax} \cos \Psi' \, dx' \, d\Psi' \tag{110}$$

and

$$E_\Phi = \frac{jk\rho}{4\pi} e^{jk\rho} \iint [\frac{e^{-jk|R_1|} e^{jk\rho \cos \Psi'}}{|R_1|}][E_{ax}] \cdot$$

$$[\sin \Theta \sin \Psi' - \cos \Psi' \sin \Phi \ (1 + \cos \Theta)] \, dx' \, d\Psi' . \tag{111}$$

A similar derivation for an aperature field polarized in the y-direction yields

$$E_r = 0, \tag{112}$$

$$E_\Theta = \frac{jk\rho}{4\pi} e^{jk\rho} \iint \frac{e^{-jk|R_1|} e^{-jk\rho \cos \Psi'}}{|R_1|} [E_{ay}]$$

$$[\cos \Psi' \sin \Phi \ (1 + \cos \Theta) - \sin \Theta \sin \Psi'] \, dx' \, d\Psi' , \tag{113}$$

and

$$E_\Phi = \frac{jk\rho}{4\pi} [\cos \Phi (\cos \Theta + 1)] \iint \frac{e^{-jk|R_1|} e^{-jk\rho \cos \Psi'}}{|R_1|}$$

$$[E_{ay} \cos \Psi'] \, dx' \, d\Psi' , \tag{114}$$

where E_{ay} is the magnitude of the aperature field polarized in the y-direction.

The two sets of equations (109-111) and (112-114) when combined will produce the Far-Field expressions for any aperature field polarized in the x-y plane. If one is interested in the Far-Field patterns only, then comparison of equations (110) and (111) to equations (113) and (114), respectively, indicates that the normalized Far-Field patterns are identical for any aperature field polarized in the x-y plane. Therefore, in order to obtain the Far-Field patterns, only one set of the equations need be considered.

APPENDIX C

LUNEBERG LENS RAY PATHS

```
      IMPLICIT REAL*8(A-H,R,P)
C     VARIABLES USED IN THE PROGRAM ARE:
C          C1-RAY PATH CONSTANT.
C          RMIN-CLOSEST POINT OF APPROACH OF RAY PATHS TO
C          LENS CENTER.
C          YRAY- Y-COMPONENT OF A RAY PATH POINT.
C          XRAY- X-COMPONENT OF A RAY PATH POINT.
C          R- NORMALIZED LENS RADIUS.
      REAL LABEL /'    '/
      REAL*8 TITLE(12)
C     READ TITLE TO BE TYPED AT BOTTOM OF GRAPH
      READ(5,100) TITLE
100   FORMAT(6A8)
C     FCT5 IS A FUNCTION WHICH WHEN INTEGRATED DESCRIBES
C     THE RAY PATHS THROUGH THE NORMALIZED LUNEBERG LENS.
      EXTERNAL FCT5
      DIMENSION XRAY(1100),YRAY(1100),AUX(25)
      COMMON C1
C     INITILIZE C1 FOR THE 1ST RAY.
      C1=0.9D0
      PI=3.14159265D0
C     ENTER LOOP TO OBTAIN DIFFERENT RAYS
      DO 1 I=1,9
C     CALCULATE RMIN
      RMIN=DSQRT(1.0D0-DSQRT(1.0D0-C1**2))
      R=1.0D0
      ASTP=0.0025D0
      NUM=((R-RMIN)/ASTP)+1
      RHO=DARSIN(C1)
      N=2*NUM
      K=N
      M=1
      PH=PI/2.0D0-DARSIN(DSQRT(1.0D0-C1**2))
      RR=R
      X1=R*DCOS(RHO)
3     IF(1.0.LE.X1) GO TO 2
C     CALCULATION OF RAY EXTENDING IN FRONT OF LENS.
      K=K+1
      X1=X1+0.005
      XRAY(K)=X1
      YRAY(K)=C1
      GO TO 3
C     CALL INTEGRATING SUBROUTINE TO SOLVE INTEGRAL EQ
2     CALL DQATR(RR,1.D0,0.0000001,15,FCT5,DAL,IER7,AUX)
      CALCULATE X AND Y VALUES TO BE USED IN PLOTTING RAYS
      PHI=PH+DAL
      PH2=PI-DAL
      XRAY(N)=RR*DCOS(PHI)
      YRAY(N)=RR*DSIN(PHI)
      XRAY(M)=RR*DCOS(PH2)
      YRAY(M)=RR*DSIN(PH2)
      IF(N-M.LE.1) GO TO 4
      N=N-1
      M=M+1
      RR=RR-ASTP
      GO TO 2
C     ENTER INTO CONTROL FOR PLOTING RAYS
4     IF(I.GT.1)GO TO 5
6     MOD=1
      GO TO 7
5     MOD=2
7     CALL DRAW(K,XRAY,YRAY,MOD,0,LABEL,TITLE,0,0,4,4,2,2,8,
     18,0,LAST)
      IF(MOD.NE.1)GO TO 300
      MOD=2
```

```
      GO TO 400
300   IF(I.GE.9) GO TO 350
      GO TO 400
350   MCD=3
400   DO 500J=1,K
500   YRAY(J)=-YRAY(J)
      CALL DRAW(K,XRAY,YRAY,MOD,0 ,LABEL,TITLE,0,0,4,4,2,2,8,
     18,0,LAST)
      C1=C1-0.1D0
1     CONTINUE
      STOP
      END


      FUNCTION FCT5(RAN)
C     FCT5 IS A CUNCTION WHICH WHEN INTEGRATED DESCRIBES
C     THE RAY PATHS THROUGH THE LUNEBERG LENS.
      IMPLICIT REAL *8(A-H,R,P)
      COMMON C1
      FCT5=C1/(RAN*DSQRT(-(RAN**4)+2.0D0*(RAN**2)-(C1**2)))
      RETURN
      END
```

FEED PATTERN FITTING
AND
APERATURE FIELD CALCULATIONS

```
C       THIS PROGRAM WAS DESIGNED TO FIT A LEAST SQLARE
C       POLYNOMINISL TO A NUMBER OF POINTS FOR A MEASURED
C       FEED PATTERN AND THEN PLOT THE FEED FUNCTION BY USING
C       THREE TIMES AS MANY POINTS (K2) IN ORDER TO DETECT ANY
C       EXCURSION THAT THE POLYNOMINISL FIT MAY HAVE TAKEN
C       BETWEEN TWO ADJACIENT POINTS .
        IMPLICIT REAL*8(D)
        DIMENSION DTHETA(100),DMAG(100),DA(20),DWI(80),DY(80),
       1DELY(80),A(20),DSA(20),THETA(200),EMAG(200),DTHE(100)
       2,EMA(200)
        REAL*8 DTITL(10)/10*' '/
        REAL LABEL/'      '/
        REAL*8 TITLE(12)
C       READ GRAPH TITLE
        READ(5,100) TITLE
100     FORMAT(6A8)
C       M IS THE DEGREE OF POLYNOMINIAL TO BE FITTED
C       N IS THE NUMBER OF POINTS IN THE CURVE TO BE FITTED.
        READ(5,200)M,N
200     FORMAT(I3/I2)
C       READ IN DATA POINTS-DTHETA IS THE ABSISSIA VALUE AND
C       DMAG IS THE SQUARE OF THE ORDINATE VALUE-SQUARE LAW
C       DETECTOR WAS USED TO OBTAIN DATA.
        READ(5,400) (DTHETA(I),DMAG(I),I=1,N)
        DO 60 J=1,N
60      DMAG(J)=DSQRT(DMAG(J))
400     FORMAT(F10.7,F12.6)
        DO 50 I=1,N
50      DTHE(I)=DTHETA(I)*(3.14159265D0/180.D0)
        DO 5 I=1,N
5       DWI(I)=1.0D0
C       LSQPL2 WILL CALCULATE THE LEASE SQUARE POLUNOMINIAL
C       COEFFCIENTS.
        CALL LSQPL2(N,M,DTHE   , DMAG,DWI,DY,DELY,DA,DSA,DTITL)
        L=1+IABS(M)
        DO 6 I=1,L
6       A(I)=DA(I)
        WRITE(6,300) (I,A(I),I=1,L)
300     FORMAT(' ','A(',I4,')=',F18.6)
        THET=DTHE(1)
        K2=3*N
C       CALCULATE SIZE OF STEPS TO BE USED IN PLOTTING CURVE.
        STEP=(DTHE(N)-DTHE(1))/K2
        WRITE(6,302)
302     FORMAT(' ',4X,'THET',12X,'EMAG')
        DO 3 K=1,K2
        THETA(K)=THET
        EM=A(1)
        DO 4 J=2,L
4       EM=EM+A(J)*THETA(K)**(J-1)
        EMAG(K)=EM
        WRITE(6,301) THET,EMAG(K)
301     FORMAT(' ',F10.5,5X,F10.7)
        THET=THET+STEP
3       CONTINUE
C       CALCULATE THE APERATURE FIELD STRENGTH
        DO 7 K=1,K2
        EMA(K)  =EMAG(K)*SQRT(1.0/COS(THETA(K)))
        WRITE(6,301)THETA(K),EMA(K)
7       CONTINUE
        DO 8 K=1,K2
        THETA(K)=THETA(K)*180.0/3.1415
8       CONTINUE
        CALL DRAW(K2 ,THETA,EMAG,1,0,LABEL,TITLE,20.0,0,0,3,2,
       12,6,7,1,LAST)
        CALL DRAW(K2 ,THETA,EMA ,3,0,LABEL,TITLE,20.0,0,0,3,2,
       12,6,7,1,LAST)
        STOP
```

```
END
```

PHE-COMPONENT LUNEBERG LENS PATTERNS

```
C     THIS PROGRAM WAS DESIGNED TO CALCULATE PHE-COMPONENT
C     OF THE RADIATION PATTERNS OF THE CYLINDRICAL LUNEBERG
C     LENS WITH BEAM CENTERED AT 0-DEGREES,FOR A VERTICALLY
C     POLARIZED FEED.THIS PATTERN IS IDENTICAL FOR ANY FEED
C     POLARIZATION IN THE X-Y PLANE
      IMPLICIT COMPLEX(C)
      COMPLEX CJ/(0.0,1.0)/
      M=0
C     STEP IS THE STEP-SIZE IN DEGREES BETWEEN POINTS WHERE
C     THE FIELD STRENGTH IS CALCULATED.
C     THETAI IS THE INITIAL ANGLE IN DEGREES FOR WHICH THE
C     FIELD STRENGTH IS CALCULATED.
C     THETAF IS THE FINAL ANGLE IN DEGREES FOR WHICH THE
C     FIELD STRENGTH IS CALCULATED.
C     ANGPD IS THE ANGLE IN DEGREES THAT CONTROLS THE PLANE
C     IN WHICH THE LENS PATTERNS ARE CALCULATED, IF 90
C     DEGREES THE THE E-PLANE PATTERNS ARE CALCULATED, IF
C     0-DEGREES THEN THE VERTICAL BEAM PATTERN IS CALCULAT-
C     ED.
      READ(5,2) STEP,THETAI, THETAF,ANGPD
2     FORMAT(F12.3/F12.3/F12.3/F12.3)
      PIE=3.1415926535
      ANGP=ANGPD*(PIE/180.0)
C     CALCULATE NUMBER OF STEPS ,NUM, WHICH IS ALSO THE
C     NUMBER OF POINTS TO BE PLOTTED BY SUBROUTINE DRAW.
      NUM=(THETAF-THETAI)/STEP +1
C     MO IS THE INTEGER THAT CONTROLS THE NUMBER OF PLOTS
C     TO BE PLOTTED BY DRAW  IN SUBROUTINE EPHEE.
C     RADIUS IS THE RADIUS OF THE LUNEBERG LENS.
C     FREQ IS THE FREQUENCY FOR WHICH THE PATTERNS ARE
C     CALCULATED.
C     THICK IS THE HEIGHT OR X-DIMENSION OF THE LENS.
12    READ(5,4) MO , RADIUS, FREQ,THICK
4     FORMAT(I1/F12.3/F12.3/F12.3)
      IF(MO .EQ.0)GO TO 14
      M=M+1
14    WRITE(6,5)THETAI, THETAF,STEP, RADIUS,FREQ,NUM,MO ,
     1THICK,ANGPD
5     FORMAT(' ','THETAI=',F11.6,/,' ','THETAF=',F11.6,/,'
     1 ','STEP=',F11.6,/,' ','RADIUS=',F11.6,/,' ',
     2'FREQUENCY=',F11.6,/,' ','NUM=',I6,/,' ','MO  ',I6,/'
     3,'THICK=',F11.6,/,' ','PHE=',F11.6)
      R=200.0
C     AK IS THE PROPAGATION CONSTANT.
      AK=20.0*PIE*FREQ/3.0
      CJKR=(CJ*AK*RADIUS/(4.0*PIE*R))*CEXP(CJ*AK*(RADIUS-R))
C     CJKRN IS THE NORMALIZED COEFFICIENTS
      CJKRN=CJKR/CABS(CJKR)
      WRITE(6,100)CJKRN
100   FORMAT(' ','CJKRN=',F11.9,2X,'J',F11.9)
      CALL EPHEE(AK,THICK,ANGP,THETAI,STEP, NUM,CJKRN,RADIUS
     1,MO ,FREQ,M)
C     EPHEE WILL CALCULATE AND PLOT THE PHE-COMPONENTS
C     OF THE E-FIELD OF THE LUNEBURG LENS
      IF(MO .EQ.0)GO TO 13
13    STOP
      END


      SUBROUTINE EPHEE (AK1,THI,ANGP1,ANGTI,STE,NUM,CJKRN,
     1RA,MOD,FRE,M1)
C     THIS SUBROUTINE WAS WRITTEN TO CALCULATE AND PLOT
C     THE PHE-COMPONENT OF THE ELECTRIC FIELD OF THE LUNE-
C     BERG LENS FOR ANY FEED FUNCTION OR ANY MEASURED FEED
C     DISTRIBUTION THAT CAN BE APPROXIMATED BY A CURVE
C     FITTING TECHNIQUE.
      IMPLICIT COMPLEX(C)
C     THE NEXT FOUR STATEMENTS CONTROL THE LABELING AND
```

```
C       TITLING OF THE GRAPHS PLOTTED BY SUBROUTINE DRAW.
        REAL LABEL /'     '/
        REAL *8 TITLE(12)
        READ(5,100) TITLE
100     FORMAT(6A8)
        COMPLEX CJ/(0.0,1.0)/
        EXTERNAL CFCT1,CFCT3
C       CFCT1 IS A FUNCTION DESCRIBING THE FAR FIELD OF THE
C       LUNEBERG LENS IN TERMS OF THE APPERATURE FIELD
C       DISTRIBUTION IN THE X-DIRECTION.
C       CFCT3 IS A FUNCTION DESCRIBING THE FAR FIELD OF THE
C       LUNEBERG LENS IN TERMS OF THE APPERATURE FIELD
C       DISTRIBUTION AS A FUNCTION OF THE
C       ANGULAR DISPLACEMENT FROM BEAM CENTER.
        DIMENSION THETA(400),CEPHE(400),EPHEM(400),RADI(5),
       1FREQ(5)
        COMMON/ALIM/ALIM1,ALIM2,THIC
        COMMON AK,ANGP,THETR,RAD,L3,L1
        THIC=THI
        RAD=RA
        RADI(M1)=RA
        FREQ(M1)=FRE
        AK=AK1
        ANGP=ANGP1
        PIE=3.14159265358
        THET=ANGTI
        TH2=-THI/2.0
        TH3=THI/2.0
        ANORM=0.0
C       ANORM IS A  VARIABLE USED TO NORMALIZE THE ELECTRIC
C       FIELD STRENGTH.
C       ENTER LOOP TO CALCULATE THE E-FIELD FOR NUM-POINTS
        DO 1 I=1,NUM
        L1=I
        L3=I
        THETR=THET*(PIE/180.0)
        CALL CWEDF(CFCT1,TH2,TH3,15,CEPH1)
        L1=2
900     XL=ALIM1
        XU=ALIM2
        CALL CWEDF(CFCT3, XL , XU ,375,CEPH3)
        IF(L3.NE.-1) GO TO 1000
        L3=2
        GO TO 900
1000    CEPH=CEPH1*CEPH3
        IF(ANORM.GE.CABS(CEPH)) GO TO 2
        ANORM=CABS(CEPH)
2       THETA(I)=THET
        CEPHE(I)=CEPH
        THET=THET+STE
1       CONTINUE
C       ENTER LOOP TO NORMALIZE AND CALCULATE THE MAGNITUDE
C       OF THE E-FIELD (EPHEM).
        DO 3 J=1,NUM
        CEPHE(J)=CEPHE(J)/ANORM
        EPHEM(J)=CABS(CEPHE(J))
3       CONTINUE
        WRITE(6,84)RADI(M1),FREQ(M1)
84       FORMAT('1','PHE-COMPONENT OF THE E-FIELD FOR LENS',
       1'RADIUS OF',F8.4,2X,'METERS AT',F8.3,2X,'GHZ',//' ',6X
       2,'THETA',12X,'FIELD STRENGTH',10X,'COMPLEX FIELD ',
       3'STRENGTH')
        J=0
        DO 23 I=1,NUM
        WRITE (6,85)THETA(I),EPHEM(I),CEPHE(I)
85      FORMAT(' ',F11.3,8X,F14.6,12X,F10.6,F10.6)
        J=J+1
        IF(J.LT.72)GO TO 23
        WRITE(6,84)RAD,FRE
        J=0
23      CONTINUE
C       ENTER LOOP TO CALCULATE THE FIELD MAGNITUDES IN DECI-
```

```
C     BELS.
      DO 20 I=1,NUM
      EPHEM(I)=20.0*ALOG10(EPHEM(I))
20    CONTINUE
      CALL DRAW(NUM,THETA,EPHEM,MOD,0,LABEL,TITLE,0,8.0,7,3,
     12,2,6,8,1,LAST)
90    RETURN
      END


      SUBROUTINE CWEDF (CF,XL,XU,NX,CANS)
C     CWEDF WAS OBTAINED FROM LCDR. E.G.NEELY .
C        CWEDF IS A SUBROUTINE WHICH WILL NUMERICALLY
C     INTEGRATE A USER SUPPLIED FUNCTION BETWEEN SPECIFIED
C     LIMITS.(SINGLE PRECISION)
C          CF    - NAME OF FUNCTION SUBPROGRAM.  MUST BE
C     LISTED IN AN EXTERNAL STATEMENT.
C          XL    - LOWER LIMIT OF INTEGRATION
C          XU    - UPPER LIMIT OF INTEGRATION
C         NX    -APPROXMATE NUMBER OF NODES AT WHICH TO
C     EVALUATE THE FUNCTION.
C          CANS - RESULT OF INTEGRATION
C
      IMPLICIT COMPLEX*8 (C)
      REAL*8 DXDX,XX
      REAL*4 CW(6)/82.,216.,27.,272.,27.,216./
      COMMON AK,ANGP,THETR,RAD,L3,L1
      IF(NX.LE.0) GO TO 900
      N=((NX+4)/6)*6+1
      DX=(XU-XL)/FLOAT(N-1)
      DXDX=DBLE(DX)
      NWIX=N/6
      X=XL
      CANS=-CF(X)*41.0
      IF(L3.EQ.-1) GO TO 1000
      IF(L1.EQ.1) GO TO 500
      IF(L3.NE.1) GO TO 500
      L3=2
500   DO 800 MX=1,NWIX
      DO 700 KX=1,6
      CANS=CANS+CW(KX)*CF(X)
      XX=DBLE(X)
      X=SNGL(XX+DXDX)
 700  CONTINUE
 800  CONTINUE
      CANS=(CANS+41.0*CF(X))*DX/140.0
      RETURN
 900  WRITE(6,901) N
 901  FORMAT('0ERROR IN CALLING PARAMETER *****   N = ',
     1I5,'   *****'//)
1000  RETURN
      END


      FUNCTION CFCT1(X)
C     CFCT1 IS A FUNCTION WHICH DESCRIBES THE FAR-FIELD
C     VARIATIONS OF THE E-FIELD AS A FUNCTION OF THE LUNE-
C     BERG LENS HEIGHT.
      IMPLICIT COMPLEX(C)
      COMPLEX CJ/(0.0,1.0)/
      COMMON AK,ANGP,THETR,RAD,L3,L1
      COMMON/ALIM/ALIM1,ALIM2,THIC
      CEX=CJ*AK*SIN(THETR)*COS(ANGP)*X
      CFCT1=CEXP(CEX)*COS(3.14159*X/THIC)
      RETURN
      END
```

```
      FUNCTION CFCT3(ANG)
C     CFCT3 IS A FUNCTION WHICH DESCRIBES THE FAR FIELD
C     VARIATIONS OF THE E-FIELD AS A FUNCTION OF ANG
C     (THE ANGLE FROM BEAM CENTER). TO DO THIS LSQPL2 IS
C     UTILIZED TO FIT A CURVE TO THE MEASURED FEED FUNCTION
C     AND COMBINES THIS WITH THE OTHER ANGULAR VARIATIONS
C     OF THE FAR-FIELD EQUATIONS.
      IMPLICIT REAL*8(D)
      IMPLICIT COMPLEX (C)
      COMPLEX CJ/(0.0,1.0)/
      DIMENSION DTHETA(100),DMAG(100),DA(20),DWI(80),DY(80),
     1DELY(80),A(20),DSA(20),THETA(100),EMAG(100),DTHE(100)
      REAL*8 DTITL(10)/10*' '/
      COMMON AK,ANGP,THETR,RAD,L3,L1
      COMMON/ALIM/ALIM1,ALIM2,THIC
C     L3 WILL BE EQUAL TO 1 ON THE FIRST CALL OF CFCT3
C     AND WILL PROCEED THROUGH THE NEXT STEPS DOWN TO 600
C     IN ORDER TO CALCULATE THE POLYNOMINIAL COEF. THAT
C     DESCRIBE THE FEED FUNCTION.
C     IF L3 IS NOT 1, THEN THE POLYNOMINIAL COEF. HAVE BEEN
C     CALCULATED BY A PREVIOUS PASS.
      IF(L3.NE.1) GO TO 600
      READ(5,200) M,N
200   FORMAT(I3/I2)
      READ(5,400) (DTHETA(I),DMAG(I),I=1,N)
400   FORMAT(F10.7,F12.6)
      DO 60 J=1,N
60    DMAG(J)=DSQRT(DMAG(J))
      DO 50 I=1,N
50    DTHE(I)=DTHETA(I)*(3.14159265D0/180.D0)
      ALIM1=DTHE(1)
      ALIM2=DTHE(N)
      DO 5 I=1,N
5     DWI(I)=1.0D0
      CALL LSQPL2(N,M,DTHE   , DMAG,DWI,DY,DELY,DA,DSA,DTITL)
      L=1+IABS(M)
      DO 6 I=1,L
      A(I)=DA(I)
6     THETA(I)=DTHETA(I)
      WRITE(6,300) (I,A(I),I=1,L)
300   FORMAT(' ','A(',I4,')=',F18.6)
      L3=-1
      RETURN
600   EM=A(1)
      DO 4 J=2,L
4     EM=EM+A(J)*ANG**(J-1)
C     EA1 IS A FUNCTION WHICH DESCRIBES THE FEED VARIATIONS
C     OVER THE PLANE OF THE LENS.
      EA1=EM
      CER=CJ*AK*RAD*(COS(ANG)*(COS(THETR)-1.0)-SIN(ANG)*
     1SIN(THETR)*SIN(ANGP))
C     THE SQRT(1.0/COS(ANG)) TERM IS THE ONLY PART OF THIS
C     EQUATION ASSOCIATED WITH THE LENS FUNCTION.
C     THE REMAINDER IS FROM THE APPLICATION OF THE APERATURE
C     FIELD METHOD TO THE SEMI-CIRCULAR APERATURE.TO MOD-
C     IFY THIS PROGRAM TO PREDICT THE CONSTANT-K LENS FAR
C     FIELD PATTERNS CHANGE THIS FUNCTION. THE CORRECT PHASE
C     TERMS ARE ALREADY INCLUDED.
      CFCT3=CEXP(CER)*(SIN(THETR)*SIN(ANG)-COS(ANG)*
     1SIN(ANGP)*(COS(THETR)+1.0))*SQRT(1.0/COS(ANG))*EA1
      RETURN
      END
```

THETA-COMPONENT LUNEBERG LENS PATTERNS

```
C     THIS PROGRAM WAS DESIGNED TO CALCULATE THE THETA COM-
C     PONENT OF THE CYLINDRICAL LUNEBERG LENS RADIATION PAT-
C     TERNS WITH BEAM CENTERED AT 0-DEGREES,FOR ANY FEED
C     POLARIZED IN THE X-Y PLANE.
      IMPLICIT COMPLEX(C)
      COMPLEX CJ/(0.0,1.0)/
      M=0
C     STEP IS THE STEP-SIZE IN DEGREES BETWEEN POINTS WHERE
C     THE FIELD STRENGTH IS CALCULATED.
C     THETAI IS THE INITIAL ANGLE IN DEGREES FOR WHICH THE
C     FIELD STRENGTH IS CALCULATED.
C     THETAF IS THE FINAL ANGLE IN DEGREES FOR WHICH THE
C     FIELD STRENGTH IS CALCULATED.
C     ANGPD IS THE ANGLE IN DEGREES THAT CONTROLS THE PLANE
C     IN WHICH THE LENS PATTERNS ARE CALCULATED, IF 90
C     DEGREES THE E-PLANE PATTERNS ARE CALCULATED,IF
C     0-DEGREES THEN THE VERTICAL BEAM PATTERN IS CALCULAT-
C     ED.
      READ(5,2) STEP,THETAI, THETAF,ANGPD
2     FORMAT(F12.3/F12.3,F12.3/F12.3)
      PIE=3.1415926535897
      ANGP=ANGPD*(PIE/180.0)
C     CALCULATE NUMBER OF STEPS REQUIRED WHICH IS THE SAME
C     AS THE NUMBER OF POINTS TO BE PLOTTED BY DRAW
      NUM=(THETAF-THETAI)/STEP +1
C     MO IS THE INTEGER THAT CONTROLS THE NUMBER OF PLOTS
C     TO BE PLOTTED BY DRAW  IN SUBROUTINE ETHETA
C     RADIUS IS THE RADIUS OF THE LUNEBERG LENS.
C     FREQ IS THE FREQUENCY FOR WHICH THE PATTERNS ARE
C     CALCULATED.
C     THICK IS THE HEIGHT OF THE LENS.
12    READ(5,4) MO , RADIUS, FREQ,THICK
4     FORMAT(I1/F12.3/F12.3/F12.3)
      IF(MO .EQ.0)GO TO 14
      M=M+1
14    WRITE(6,5)THETAI, THETAF,STEP, RADIUS,FREQ,NUM,MO,
     1THICK,ANGPD
5     FORMAT(' ','THETAI=',F11.3,/,' ','THETAF=',F11.3,/,
     1' ','STEP=',F11.6,/,' ','RADIUS=',F11.6,/,' ',
     2'FREQUENCY=',F11.6,/,' ','NUM=',I6,/,' ','MO =,',I6
     3,/' ','THICK=',F11.6,/' ','PHE=',F11.6)
      R=200.0
C     AK IS THE PROPAGATION CONSTANT.
      AK=20.0*PIE*FREQ/3.0
      CJKR=(CJ*AK*RADIUS/(4.0*PIE*R))*CEXP(CJ*AK*(RADIUS-R))
      CJKRN=CJKR/CABS(CJKR)
      WRITE(6,100)CJKRN
100   FORMAT(' ','CJKRN=',F11.9,2X,'J',F11.9)
      CALL ETHETA(AK,THICK,ANGP,THETAI,STEP,NUM,CJKRN,RADIUS
     1MO ,FREQ,M)
C     EHTETA WILL CALCULATE AND PLOT THE THETA COMPONENTS
C     -FIELD PATTERNS OF THE  LUNEBURG LENS
      IF(MO .EQ.0)GO TO 13
13    STOP
      END


      SUBROUTINE ETHETA(AK1,THI,ANGP1,ANGTI,STE,NUM,CJKRN,
     1RA,MOD,FRE,M1)
C     THIS SUBROUTINE WAS WRITTEN TO CALCULATE AND PLOT
C     THE THETA-COMPONENT OF THE ELECTRIC FIELD OF THE LUNE-
C     BERG LENS FOR ANY FEED FUNCTION OR ANY MEASURED FEED
C      DISTRIBUTION THAT CAN BE APPRIXIMATED BY A CURVE
C      FITTING TECHNIQUE.
      IMPLICIT COMPLEX(C)
C     THE NEXT FOUR STATEMENTS CONTROL THE LABELING AND
C     TITLING OF THE GRAPHS PLOTTED BY SUBROUTINE DRAW.
      REAL LABEL /'    '/
```

```
      REAL *8 TITLE(12)
      READ(5,100) TITLE
100   FORMAT(6A8)
      COMPLEX CJ/(0.0,1.0)/
C     CFCT1 IS A FUNCTION DESCRIBING THE FAR FIELD OF THE
C     LUNEBERG LENS IN TERMS OF THE APPERATURE FIELD
C     DISTRIBUTION IN THE X-DIRECTION.
C     CFCT4 IS A FUNCTION DESCRIBING THE FAR FIELD OF THE
C     LUNEBERG LENS IN TERMS OF THE APPERATURE FIELD
C     DISTRIBUTION AS A FUNCTION OF THE
C     ANGULAR DISPLACEMENT FROM BEAM CENTER.
      EXTERNAL CFCT1,CFCT4
      DIMENSION THETA(400),CETHE(400),ETHEM(400),RADI(5),
     1FREQ(5)
      COMMON AK,ANGP,THETR,RAD,L3,L1
      COMMON/ALIM/ALIM1,ALIM2,THIC
      THIC=THI
      RAD=RA
      RADI(M1)=RA
      FREQ(M1)=FRE
      AK=AK1
      ANGP=ANGP1
      PIE=3.141592653589
      THET=ANGTI
      TH2=-THI/2.0
      TH3=THI /2.0
      ANORM=0.0
C     ENTER LOOP TO CALCULATE THE E-FIELD FOR NUM-POINTSIN
      DO 1 I=1,NUM
      L1=I
      L3=I
      THETR=THET*(PIE/180.0)
      CALL CWEDF(CFCT1,TH2,TH3,5,CETH1)
      L1=2
900   XL=ALIM1
      XU=ALIM2
      CALL CWEDF(CFCT4, XL   , XU   ,375,CETH4)
      IF(L3.NE.-1) GO TO 1000
      L3=2
      GO TO 900
1000  CETH=CETH1*CETH4
      WRITE(6,96) CETH1,CETH4,CETH
96    FORMAT(' ',6E12.6)
C     WRITE(6,15)CETH
15    FORMAT(' ','CETH=',2F10.5)
      IF(ANORM.GE.CABS(CETH)) GO TO 2
      ANORM=CABS(CETH)
2     THETA(I)=THET
      CETHE(I)=CETH
      THET=THET+STE
      WRITE(6,95) THET,ANORM
95    FORMAT(' ',2F12.5)
1     CONTINUE
C     ENTER LOOP TO NORMALIZE AND CALCULATE THE MAGNITUDE
C     OF THE E-FIELD (EPHEM).
      DO 3 J=1,NUM
      CETHE(J)=CETHE(J)/ANORM
      ETHEM(J)=CABS(CETHE(J))
3     CONTINUE
      WRITE(6,84)RADI(M1),FREQ(M1)
84     FORMAT('1','THETA-COMPONENT OF THE E-FIELD FOR LENS',
     1'RADIUS OF',F8.4,2X,'METERS AT',F8.4,2X,'GHZ',//' ',6X
     2,'THETA',12X,'FIELD STRENGTH',10X,'COMPLEX FIELD ',
     3'STRENGTH')
      J=0
      DO 23 I=1,NUM
      WRITE (6,85)THETA(I),ETHEM(I),CETHE(I)
85    FORMAT(' ',F11.3,8X,F14.6,12X,F10.6,F10.6)
      J=J+1
      IF(J.LT.72)GO TO 23
      WRITE(6,84)RAD,FRE
      J=0
```

```
23    CONTINUE
C     ENTER LOOP TO CALCULATE THE FIELD MAGNITUDES IN DECI-
C     BELS.
      DO 20 I=1,NUM
      ETHEM(I)=20.0*ALOG10(ETHEM(I))
20    CONTINUE
      CALL DRAW(NUM,THETA,ETHEM,MOD,0,LABEL,TITLE,0,0,7,3,2,
     12,6,8,1,LAST)
90    RETURN
      END


      SUBROUTINE CWEDF (CF,XL,XU,NX,CANS)
C
C     CWEDF WAS OBTAINED FROM LCDR. E.G.NEELY .
C        CWEDF IS A SUBROUTINE WHICH WILL NUMERICALLY
C     INTEGRATE A USER SUPPLIED FUNCTION BETWEEN SPECIFIED
C     LIMITS.(SINGLE PRECISION)
C          CF    - NAME OF FUNCTION SUBPROGRAM.  MUST BE
C     LISTED IN AN EXTERNAL STATEMENT.
C          XL    - LOWER LIMIT OF INTEGRATION
C          XU    - UPPER LIMIT OF INTEGRATION
C         NX    -APPROXMATE NUMBER OF NODES AT WHICH TO
C     EVALUATE THE FUNCTION.
C          CANS - RESULT OF INTEGRATION
C
      IMPLICIT COMPLEX*8 (C)
      REAL*8 DXDX,XX
      REAL*4 CW(6)/82.,216.,27.,272.,27.,216./
      COMMON AK,ANGP,THETR,RAD,L3,L1
      IF(NX.LE.0) GO TO 900
      N=((NX+4)/6)*6+1
      DX=(XU-XL)/FLOAT(N-1)
      DXDX=DBLE(DX)
      NWIX=N/6
      X=XL
      CANS=-CF(X)*41.0
      IF(L3.EQ.-1) GO TO 1000
      IF(L1.EQ.1) GO TO 500
      IF(L3.NE.1)GO TO 500
      L3=2
500   DO 800 MX=1,NWIX
      DO 700 KX=1,6
      CANS=CANS+CW(KX)*CF(X)
      XX=DBLE(X)
      X=SNGL(XX+DXDX)
 700  CONTINUE
 800  CONTINUE
      CANS=(CANS+41.0*CF(X))*DX/140.0
      RETURN
 900  WRITE(6,901) N
 901  FORMAT('0ERROR IN CALLING PARAMETER *****   N = ',
     1I5,'  *****'//)
1000  RETURN
      END
      COMPLEX FUNCTION CFCT1(X)
C     CFCT1 IS A FUNCTION WHICH DESCRIBES THE FAR-FIELD
C     VARIATIONS OF THE E-FIELD AS A FUNCTION OF THE LUNE-
C     BERG LENS HEIGHT.
      IMPLICIT COMPLEX(C)
      COMPLEX CJ/(0.0,1.0)/
      COMMON AK,ANGP,THETR,RAD,L3,L1
      COMMON/ALIM/ALIM1,ALIM2,THIC
      CEX=CJ*AK*SIN(THETR)*COS(ANGP)*X
      CFCT1=CEXP(CEX)*COS(X*3.14159/THIC)*(1.0+COS(THETR))*
     1COS(ANGP)
      RETURN
      END
      COMPLEX FUNCTION CFCT4(ANG)
C     CFCT4 IS A FUNCTION WHICH DESCRIBES THE FAR FIELD
C     VARIATIONS OF THE E-FIELD AS A FUNCTION OF ANG
C     (THE ANGLE FROM BEAM CENTER). TO DO THIS LSQPL2 IS
```

```
C     UTILIZED TO FIT A CURVE TO THE MEASURED FEEC FUNCTION
C     AND COMBINES THIS WITH THE OTHER ANGULAR VARIATIONS
C     OF THE FAR-FIELD EQUATIONS.
      IMPLICIT REAL*8(D)
      IMPLICIT COMPLEX(C)
      CCMPLEX CJ/(0.0,1.0)/
      DIMENSION DTHETA(100),DMAG(100),DA(20),DWI(80),DY(80),
     1DELY(80),A(20),DSA(20),THETA(100),EMAG(10C),DTHE(100)
      REAL*8 DTITL(10)/10*'  '/
      CCMMON AK,ANGP,THETR,RAD,L3,L1
      CCMMON/ALIM/ALIM1,ALIM2,THIC
C     L3 WILL BE EQUAL TC 1 ON THE FIRST CALL OF CFCT4
C     AND WILL PROCEED THROUGH THE NEXT STEPS DCWN TO 600
C     IN ORDER TO CALCULATE THE POLYNOMINIAL COEF. THAT
C     DESCRIBE THE FEED FUNCTION.
C     IF L3 IS NOT 1, THEN THE POLYNOMINIAL COEF. HAVE BEEN
C     CALCULATED BY A PREVIOUS PASS.
      IF(L3.NE.1)GO TO 600
      READ(5,200)M,N
200   FCRMAT(I3/I2)
      READ(5,40C)(DTHETA(I),DMAG(I),I=1,N)
400   FORMAT(F10.7,F12.6)
      DO 60 J=1,N
60    DMAG(J)=DSQRT(DMAG(J))
      DC 50 I=1,N
50    DTHE(I)=DTHETA(I)*(3.14259265D0/180.0D0)
      ALIM1=DTHE(1)
      ALIM2=DTHE(N)
      DO 5 I=1,N
5     DWI(I)=1.0D0
      CALL LSQPL2(N,M,DTHE,DMAG,DWI,DY,CELY,DA,CSA,DTITL)
      L=1-M
      DO 6 I=1,L
      A(I)=DA(I)
6     THETA(I)=DTHETA(I)
      WRITE(6,300)(I,A(I),I=1,L)
300   FCRMAT(' ','A(',I4,')=',F18.6)
      L3=-1
      RETURN
600   EM=A(1)
      DO 4 J=2,L
      ANGE=ANG**(J-1)
      IF(ABS(ANGE).LT.10.E-70) GO TO 7
4     EM=EM+A(J)*ANGE
C     EA1 IS A FUNCTION WHICH DESCRIBES THE FEED VARIATIONS
C     OVER THE PLANE OF THE LENS.
7     EA1=EM
      CER=CJ*AK*RAD*(COS(ANG)*(COS(THETR)-1.0)-SIN(ANG)*
     1SIN(THETR)*SIN(ANGP))
C     THE SQRT(1.0/COS(ANG)) TERM IS THE ONLY PART OF THIS
C     EQUATION ASSOCIATED WITH THE LENS FUNCTICN.
3     THE REMAINDER IS FROM THE APPLICATION OF THE APERATURE
C     FIELD METHOD TO THE SEMI-CIRCULAR APERATURE.TO MOD-
C     IFY THIS PROGRAM TO PREDICT THE CONSTANT-K LENS FAR
C     FIELD PATTERNS CHANGE THIS FUNCTICN. THE CCRRECT PHASE
C     TERMS ARE ALREADY INCLUDED.
      CFCT4=CEXP(CER)*EA1*SQRT(COS(ANG))
      RETURN
      END
```

BIBLIOGRAPHY

1. Luneberg, R.K., The Mathematical Theory of Optics, Brown University Press, 1944.
2. Bryant, M.B. and Hunt B.R., "Luneberg Lens Antenna Testing for ECM Application," Naval Electronics Laboratory Center, 1 April 1969.
3. Born and Wolf, Principles of Optics, Pergamon Press, 1970.
4. Peeler, G.M.D., and Archer, D.H., "A Two Dimensional Microwave Luneberg Lens," IRE Transactions on Antennas and Propagation, July 1953, pp.
5. Walters, C.H., Traveling Wave Antennas, McGraw-Hill, 1965.

INITIAL DISTRIBUTION LIST

		No. Copies
1.	Defense Documentation Center Cameron Station Alexandria, Virginia 22314	2
2.	Library, Code 0212 Naval Postgraduate School Monterey, California 93940	2
3.	Dr. Richard W. Adler (thesis advisor) Department of Electrical Engineering - code 52Ab Naval Postgraduate School Monterey, California 93940	1
4.	LT Robert B. Birchfield 613 South Perry Street Attica, Indiana 47918	1
5.	Dr. R.C. Hansen 17100 Ventura Blvd. Encino, California 91316	1
6.	Director, Naval Research Center Washington D.C. 20375 ATTN: Charles T. Bender	1
7.	Commanding Officer Naval Electronic Laboratory Center 271 Catalina Blvd. San Diego, California 92152 ATTN: M.B. Bryant	1

UNCLASSIFIED

SECURITY CLASSIFICATION OF THIS PAGE (*When Data Entered*)

REPORT DOCUMENTATION PAGE		READ INSTRUCTIONS BEFORE COMPLETING FORM
1. REPORT NUMBER	2. GOVT ACCESSION NO.	3. RECIPIENT'S CATALOG NUMBER
4. TITLE (*and Subtitle*) The Far Field Analysis of Parallel Plate Luneberg Lenses for Various Feeds		5. TYPE OF REPORT & PERIOD COVERED Master's Thesis; September 1973
		6. PERFORMING ORG. REPORT NUMBER
7. AUTHOR(*s*) Robert Boyd Birchfield		8. CONTRACT OR GRANT NUMBER(*s*)
9. PERFORMING ORGANIZATION NAME AND ADDRESS Naval Postgraduate School Monterey, California 93940		10. PROGRAM ELEMENT, PROJECT, TASK AREA & WORK UNIT NUMBERS
11. CONTROLLING OFFICE NAME AND ADDRESS Naval Postgraduate School Monterey, California 93940		12. REPORT DATE September 1973
		13. NUMBER OF PAGES
14. MONITORING AGENCY NAME & ADDRESS(*if different from Controlling Office*) Naval Postgraduate School Monterey, California 93940		15. SECURITY CLASS. (*of this report*) Unclassified
		15a. DECLASSIFICATION/DOWNGRADING SCHEDULE

16. DISTRIBUTION STATEMENT (*of this Report*)

Approved for public release; distribution unlimited.

17. DISTRIBUTION STATEMENT (*of the abstract entered in Block 20, if different from Report*)

18. SUPPLEMENTARY NOTES

19. KEY WORDS (*Continue on reverse side if necessary and identify by block number*)

Luneberg Lens
Aperature Field
Far Field Radiation
Microwave Antenna

20. ABSTRACT (*Continue on reverse side if necessary and identify by block number*)

This thesis developed expressions for the aperature fields and integral equations for the far field radiation characteristics of the Parallel Plate Luneberg Lens Microwave Antenna operating in the TEM or TE_{10} modes. These expressions were programmed on a difital computer to predict the far field radiation patterns for several feed systems. Experimentation produced far field radiation patterns that were very close to the theoretical patterns for the TE_{10} mode lens and substantially different for the TEM mode lens.

DD FORM 1 JAN 73 1473 EDITION OF 1 NOV 65 IS OBSOLETE
(Page 1) S/N 0102-014-6601 |

UNCLASSIFIED

SECURITY CLASSIFICATION OF THIS PAGE (*When Data Entered*)

DD Form 1473 (BACK)
1 Jan 73
S/N 0102-014-6601

Thesis 146097
B5434 Birchfield
c.1 The far field analysis of parallel plate Luneberg Lenses for various feeds.

Thesis 146097
B5434 Birchfield
c.1 The far field analysis of parallel plate Luneberg Lenses for various feeds.

thesB5434
The far field analysis of parallel plate
3 2768 001 03656 9
DUDLEY KNOX LIBRARY